



**HAL**  
open science

## **vLIP, a viral lipase homologue, is a virulence factor of Marek's disease virus**

Jeremy P Kamil, B. Karsten Tischer, Sascha Trapp, Venugopal K Nair,  
Nikolaus Osterrieder, Hsing-Jien Kung

► **To cite this version:**

Jeremy P Kamil, B. Karsten Tischer, Sascha Trapp, Venugopal K Nair, Nikolaus Osterrieder, et al..  
vLIP, a viral lipase homologue, is a virulence factor of Marek's disease virus. *Journal of Virology*,  
2005, 79 (11), pp.6984-6996. 10.1128/JVI.79.11.6984-6996.2005 . hal-02680358

**HAL Id: hal-02680358**

**<https://hal.inrae.fr/hal-02680358>**

Submitted on 31 May 2020

**HAL** is a multi-disciplinary open access archive for the deposit and dissemination of scientific research documents, whether they are published or not. The documents may come from teaching and research institutions in France or abroad, or from public or private research centers.

L'archive ouverte pluridisciplinaire **HAL**, est destinée au dépôt et à la diffusion de documents scientifiques de niveau recherche, publiés ou non, émanant des établissements d'enseignement et de recherche français ou étrangers, des laboratoires publics ou privés.

## vLIP, a Viral Lipase Homologue, Is a Virulence Factor of Marek's Disease Virus

Jeremy P. Kamil,<sup>1,2</sup> B. Karsten Tischer,<sup>1</sup> Sascha Trapp,<sup>1</sup> Venugopal K. Nair,<sup>3</sup>  
Nikolaus Osterrieder,<sup>1\*</sup> and Hsing-Jien Kung<sup>2</sup>

*Department of Microbiology and Immunology, College of Veterinary Medicine, Cornell University, Ithaca, New York 14853<sup>1</sup>;  
Department of Biological Chemistry, School of Medicine, University of California at Davis, UC Davis Cancer Center,  
Sacramento, California 95817<sup>2</sup>; and Viral Oncogenesis Group, Institute for Animal Health,  
Compton, Berkshire, United Kingdom<sup>3</sup>*

Received 28 October 2004/Accepted 6 January 2005

**The genome of Marek's disease virus (MDV) has been predicted to encode a secreted glycoprotein, vLIP, which bears significant homology to the  $\alpha/\beta$  hydrolase fold of pancreatic lipases. Here it is demonstrated that MDV vLIP mRNA is produced via splicing and that vLIP is a late gene, due to its sensitivity to inhibition of DNA replication. While vLIP was found to conserve several residues essential to hydrolase activity, an unfavorable asparagine substitution is present at the lipase catalytic triad acid position. Consistent with structural predictions, purified recombinant vLIP did not show detectable activity on traditional phospholipid or triacylglyceride substrates. Two different vLIP mutant viruses, one bearing a 173-amino-acid deletion in the lipase homologous domain, the other having an alanine point mutant at the serine nucleophile position, caused a significantly lower incidence of Marek's disease in chickens and resulted in enhanced survival relative to two independently produced vLIP revertants or parental virus. These data provide the first evidence that vLIP enhances the replication and pathogenic potential of MDV. Furthermore, while vLIP may not serve as a traditional lipase enzyme, the data indicate that the serine nucleophile position is nonetheless essential in vivo for the viral functions of vLIP. Therefore, it is suggested that this particular example of lipase homology may represent the repurposing of an  $\alpha/\beta$  hydrolase fold toward a nonenzymatic role, possibly in lipid bonding.**

Marek's disease virus (MDV) is a widespread alphaherpesvirus of poultry that is capable of causing a fatal lymphoproliferative disease within 2 to 3 weeks of infection. The virus is highly cell associated and undergoes a major burst of replication in B lymphocytes during primary infection (17, 19). Latency occurs in CD4<sup>+</sup> T cells, and characteristic disease symptoms occur when a subset of latently infected T cells become transformed and invade nervous tissues and various organs, often resulting in paralysis and death in affected birds (17, 19). The virus is shed from the feather follicle, and inhalation of contaminated feather dander is the likely route of infection (18). Economic losses have been largely controlled by vaccination (19). However, vaccination per se does not prevent superinfection, and emergent MDV strains have been known to cause Marek's disease (MD) in vaccinated chickens (83, 84). The genome of MDV-1, as well as those of both of the other members of the Marek's disease-like genus of herpesviruses, has been sequenced (3, 41, 46, 49, 78), and the contributions of some of the specific genes involved in the pathogenesis of MDV are beginning to be addressed (26, 53, 63, 65).

Amino acid homology to lipases was originally detected in an open reading frame (ORF) of the MDV genome during the examination of sequence data from the unique long (U<sub>L</sub>) region of the GA strain (49). The ORF in question, originally designated LORF2, was hence termed "viral lipase," or vLIP (49). The vLIP reading frame is conserved among all three

members of the Marek's disease-like virus genus (3, 41, 46, 49, 78), and homologues are also found in certain avian adenoviruses (20, 23, 37, 59, 80). The complete vLIP ORF is 756 amino acids in length, and significant homology to pancreatic lipases is found in a stretch of approximately 141 amino acids that span positions 229 to 369. This 141-amino-acid region of vLIP shows 41% similarity (23% identity) to a wasp phospholipase A<sub>1</sub> (*Polistes annularis*) and 42% similarity (26% identity) to a rodent pancreatic lipase (*Myocastor coypus*). Importantly, this region corresponds to the core of the pancreatic lipase  $\alpha/\beta$  hydrolase fold, containing the Ser-Asp-His catalytic triad, which confers enzyme activity in this class of enzymes (70). Moreover, the serine nucleophile position of the vLIP catalytic triad is found in the context of a characteristic GX<sub>2</sub>SXG motif (70). In solved structures of pancreatic lipases, this catalytic serine is located in a sharp turn in the primary amino acid chain between a  $\beta$ -strand and an  $\alpha$ -helix (12, 71, 81, 82).

Lipases are water-soluble enzymes that catalyze the hydrolysis of ester bonds in water-insoluble, "lipid" substrates (27, 30, 75) and perform critical roles in a wide array of biological processes ranging from routine metabolism of dietary triacylglycerides to mediation of cell signaling and immune activity (21, 29, 40, 55, 73, 77). The pancreatic lipase (PL) gene family represents a subset of the lipolytic enzymes that build their catalytic mechanism upon a variation of the  $\alpha/\beta$  hydrolase fold, a protein fold consisting of interleaving  $\alpha$ -helices and  $\beta$ -strands that has been found to mediate a myriad of diverse enzyme activities in nature (35, 61, 70). Members of the PL gene family include human pancreatic lipase (HPL), pancreatic lipase-related proteins 1 and 2 (PLRP1 and PLRP2), hepatic lipase,

\* Corresponding author. Mailing address: Department of Microbiology and Immunology, College of Veterinary Medicine, Cornell University, Ithaca, NY 14853. Phone: (607) 253-4045. Fax: (607) 253-3384. E-mail: no34@cornell.edu.

endothelial lipase, and several wasp venom phospholipases (21). With the notable exception of the wasp venom phospholipases, which act exclusively on phospholipid substrates, PL gene family members hydrolyze the A<sub>1</sub> and A<sub>3</sub> positions of triacylglyceride substrates and show varying degrees of activity on the A<sub>1</sub> position of phospholipid substrates (21). There are other  $\alpha/\beta$  hydrolase fold lipases that are not members of the PL gene family; these include the gastric lipases and several fungal lipases (35, 56, 70). Moreover, there are several important cellular lipase activities, including phospholipases A<sub>2</sub>, C, and D, which are not mediated by  $\alpha/\beta$  hydrolases.

Although no herpesviruses outside the Marek's disease-like genus have been reported to encode proteins with homology to lipases, it is worth noting that there has been some precedent for lipases encoded by DNA viruses. A phospholipase A<sub>2</sub> activity of a parvovirus capsid protein is reportedly essential for viral infectivity (33). The p37 glycoprotein of vaccinia virus bears homology to phospholipase D enzymes, and bona fide lipase activities have been demonstrated in vitro (8). The genomes of at least two entomopoxviruses encode proteins homologous to fungal  $\alpha/\beta$  hydrolase fold lipases (2, 9). Furthermore, some DNA viruses have been demonstrated to manipulate host lipid metabolism. For example, orthopoxviruses affect both arachidonic acid and polyphosphoinositide metabolism in infected cells (60, 62). More recently, human cytomegalovirus (HCMV) has been reported to carry a host cell-derived phospholipase A<sub>2</sub> activity which is required for infectivity (5).

An MDV mutant isolated in cell culture was found to harbor a retrovirus long terminal repeat disrupting what is now known to be the *vLIP* ORF (39). This long terminal repeat insertion provided the first hint that *vLIP* is not essential for replication in vitro. Here we provide the first data to address the role of *vLIP* in vivo and also provide basic characterization of the *vLIP* transcript and gene product. We demonstrate that *vLIP* is expressed as a secreted glycoprotein from a spliced RNA, lacks detectable lipase activity in vitro, and is completely dispensable for virus replication in vitro but plays an important role in the pathogenesis of MD in the chicken.

## MATERIALS AND METHODS

**Sequence analysis and secondary-structure prediction.** BLAST and PSI-BLAST analyses of *vLIP* protein sequences were performed using National Center for Biotechnology Information servers (6, 7). Prediction of *vLIP* protein structure was performed using the GenTHREADER program via the PSIPRED server (45). For the prediction of signal peptides and signal peptide cleavage sites, the SignalP prediction server (version 1.1) was used (57, 58). Routine amino acid alignments were performed using MacVector 7.2.2 software (Accelrys, San Diego, CA) using default settings.

**Virus and cells.** The MDCC MSB-1 tumor cell line harboring latent MDV (4) was maintained in RPMI 1640 medium supplemented with 10% fetal bovine serum (FBS) at 37°C. Lytic virus replication was induced by the addition of sodium butyrate to a final concentration of 3 mM. In some experiments, 0.5 mM foscarnet (trisodium phosphonoformate hexahydrate [PFA]; Sigma-Aldrich, St. Louis, MO) was used at the time of induction to determine kinetic classes of transcripts. For the animal study and for growth of lytic MDV in culture, bacterial artificial chromosome (BAC) clones derived from the RB-1B strain of MDV (pRB-1B) were reconstituted by standard calcium phosphate transfection (72) and were passaged no more than three times for in vivo studies and no more than five times for in vitro studies. Transfection and propagation of pRB-1B-based parental, mutant, and revertant MDVs were performed on secondary chicken embryo cells (CEC), which were cultivated in a 1:1 mixture of EMEM and HMEM supplemented with 2 to 10% FBS (72).

TABLE 1. Primers and real-time PCR probes used in this study

Primer	Sequence <sup>a</sup>
SS-dT .....	5'-CGTAGGTTACCGTATCGGATAGCGGCC GCA(T) <sub>18</sub> -3'
SS .....	5'-CGTAGGTTACCGTATCGGATAGCGG-3'
spLIP5'Cpo .....	5'-CGGTCCGACCATGCCGAGTAAAAGTAT TGCGG-3'
LIP.RC(AS) .....	5'-TGAATGTCCATGATCGGCTC-3'
BamHILipS .....	5'-GGATCCTGTTATGATATTTTCAGATATT AAG-3'
XhoILipAS .....	5'-CTCGAGGACCCGGAAGTTGTGAG-3'
LipMutS .....	5'-GAATCCATTGTATGGCCATGCCTTGG GATCATATGTCTG-3'
LipMutAS .....	5'-CAGACATATGATCCCAAGGCATGGCC ATACAATGGATTC-3'
LipFLAGS .....	5'-GACTACAAGGATGACGACGATAAGTG AATCGATTTCGATAATAAAG-3'
LipFLAGS2 .....	5'-TACAAGACCGCCACCCCTAG-3'
LIPFLAGR .....	5'-CTTATCGTCGTCATCCTTGTAGTCTACC CGCGAAGTTGTGAGAGC-3'
LIPF2 .....	5'-TACTGTATTGCTCCTCCG-3'
gD probe .....	5'-FAM-CATGTTTGTCTTGGGCAGAGCA TGTG-BHQ1-3'
ck-iNOS probe .....	5'-FAM-CTCTGCCTGCTGTTGCCAACATG C-BHQ1-3'
gD F .....	5'-TGGGACGACGCAAATATGATG-3'
gD R .....	5'-AATGGTTCATTAGTAGAGCAGTTGGC-3'
ck-iNOS F .....	5'-GAGTGGTTAAGGAGTTGGATCTGA-3'
ck-iNOS R .....	5'-TTCCAGACCTCCCACCTCAA-3'

<sup>a</sup> Boldfaced and underlined nucleotides indicate the specific base pair and codon where the S307A change was incorporated into *vLIP* cDNA.

*Trichoplusia ni* insect cells, used for the expression of recombinant *vLIP*, were grown in 250-ml to 1-liter polycarbonate Erlenmeyer flasks (Nalgene) at 140 rpm in shaker culture at 28°C in ExCell 405 medium (JRH Biosciences, Lenexa, KS). *Spodoptera frugiperda* (Sf9) insect cells were grown in a similar manner to the *T. ni* cells, except that ExCell 420 medium (JRH Biosciences) was used.

**Cloning and characterization of *vLIP* mRNA.** Total RNA was isolated from 1 × 10<sup>8</sup> MSB-1 cells using Trizol (Invitrogen, Carlsbad, CA) according to the manufacturer's instructions. For cDNA synthesis, 20  $\mu$ g of total RNA was used for first-strand synthesis primed with the SS-dT oligonucleotide (Table 1). Reverse transcription (RT) was carried out using avian myeloblastosis virus reverse transcriptase (Roche, Indianapolis, IN) at 42°C for 1 h using the conditions specified by the manufacturer. Upon completion of RT, reactions were extracted against phenol-chloroform and passed over Chromaspin TE 200 columns (Stratagene Inc., La Jolla, CA).

Primers (200 nM each) used in rapid amplification of 3' cDNA ends were SS and sp.LIP5'Cpo (Table 1). Thirty PCR cycles (93°C for 45 s, 56°C for 60 s, and 68°C for 300 s) were performed, using Expand High-Fidelity *Taq* polymerase (Roche) at 2.3 U (0.7  $\mu$ l) per 50- $\mu$ l reaction volume. PCR products were cloned into the pCR2.1-TopoTA vector (Invitrogen). The LIP.RC(AS) and sp.LIP5'CPO primers were used to screen bacterial colonies for plasmids with spliced *vLIP* cDNA inserts (Table 1). DNA sequencing was performed using vector-specific primers, along with several *vLIP*-specific primers designed from MDV genomic DNA sequences (Davis Sequencing LLC, Davis, CA). All oligonucleotides were custom synthesized (Integrated DNA Technologies, Coralville, IA).

For Northern blot analysis, 10  $\mu$ g of total RNA was denatured for 15 min at 65°C, loaded onto 1% agarose-6% formaldehyde gels, and run at 75 V in 50 mM morpholinepropanesulfonic acid (MOPS) buffer (pH 7.2). Resolved RNAs were transferred overnight onto Hybond-N membranes (Amersham Biosciences Corp., Piscataway, NJ) by the capillary method in 20× SSC (1× SSC is 0.15 M NaCl plus 0.015 M sodium citrate, pH 7.0) (68). Transferred RNA was UV cross-linked using the Stratalinker apparatus (Stratagene). A <sup>32</sup>P-labeled 376-bp single-stranded RNA probe antisense to *vLIP* mRNA was transcribed in vitro from a pSP72 (Promega, Madison, WI)-based plasmid using the MaxiScript T7 kit (Ambion) after linearization of the construct. As a negative control, a sense single-stranded RNA probe corresponding to residues coding for amino acids 158 to 255 of *vLIP* was prepared and hybridized in parallel to a duplicate membrane. Unincorporated radioactivity was removed using NICK columns

(Amersham Biosciences). Membranes were hybridized overnight at 68°C in UltraHyb solution (Ambion), and  $1.5 \times 10^6$  cpm of probe per ml of hybridization solution was used in each experiment. Blots were washed twice for 5 min each at room temperature in  $2 \times$  SSC–0.1% sodium dodecyl sulfate (SDS) and twice for 15 min each at 68°C in  $0.1 \times$  SSC–0.1% SDS; then they were exposed at –80°C to BioMax MR film (Kodak, Rochester, NY) in the presence of an intensifying screen. The Millennium RNA ladder (Ambion), in conjunction with a  $^{32}$ P-labeled Millennium probe (Ambion), was used to determine RNA sizes.

**Construction of plasmids.** The QuikChange kit (Stratagene) was used to introduce an S307A change at the predicted nucleophile site of *vLIP*. According to the manufacturer's instructions, the LipMutS and LipMutAS primers (Table 1) were used to introduce a single-base-pair change from thymidine to guanine, changing a TCC serine codon to a GCC alanine codon. For baculovirus expression, wild-type (wt) *vLIP* cDNA or S307A *vLIP* cDNA, starting at residue Val31 (a predicted signal peptide comprises residues 1 to 30) was PCR adapted with BamHI and XhoI sites at the 5' and 3' ends, using primers BamHILipS and XhoILipAS (Table 1), and then inserted into pBAC11 (Novagen, Madison, WI). This cloning strategy placed the N terminus of *vLIP* cDNA in frame with the gp64 signal peptide from pBAC11 and placed the C terminus of *vLIP* in frame with a polyhistidine tag also encoded by the vector. All clones were verified by DNA sequencing.

To incorporate a FLAG epitope tag (DYKDDDDK) at the carboxy terminus of *vLIP*, overlap extension PCR was used. Separate PCRs were performed with the following pairs of primers: LIPFLAGS–LIPFLAGS2 and LIPLAGR–LIPF2 (Table 1). The resulting PCR products were purified by agarose gel electrophoresis and combined in an overlap extension PCR performed using the external primers (LIPFLAGS2 and LIPF2). The PCR product was then cloned into pCR2.1-TopoTA (Invitrogen) and sequenced (Cornell BioResource Center). A sequence-verified clone was digested with BsiWI and ClaI to release a FLAG-tagged fragment of the *vLIP* cDNA. The BsiWI–ClaI fragment was then ligated into pEco4.268, yielding pEco4.268\_*vLIP*\* (see Fig. 5). The pEco4.268 plasmid was originally constructed by inserting the EcoRI 4,268-bp subfragment of the Md5 genome derived from the sn5 cosmid (65) (a gift of Sanjay Reddy) into pUC18 (Fig. 5).

In order to construct a shuttle vector to incorporate an in-frame deletion of amino acids 256 to 428 of the *vLIP* open reading frame, a 519-bp fragment was released from the pEco4.268 plasmid using MluI and SpeI, and overhangs were filled in using T4 DNA polymerase (NEB). Finally, the plasmid was closed using T4 DNA ligase (NEB) and transformed into *Escherichia coli*. Individual plasmids bearing the deletion were sequenced, and a clone bearing an in-frame deletion was obtained and digested with the BamHI and PshAI enzymes (NEB). The 3,307-bp BamHI–PshAI fragment was inserted into pST76K-SR (1), a vector for performing RecA-based shuttle mutagenesis, which had been opened with BamHI and SmaI. To prepare a similar shuttle vector that would be used to restore the wt *vLIP* gene to the deletion mutant BAC, pEco4.268 was digested with BamHI and PshAI, and the 3,826-bp fragment was ligated into pST76K-SR as described above. In order to prepare a shuttle vector to transfer the S307A mutation into the pRB-1B BAC, a pCR2.1-*vLIP* cDNA clone bearing the S307A mutation was digested with MluI and SpeI, and the 516-bp MluI–SpeI fragment was inserted into the pEco4.268 plasmid. After confirmation of the presence of the S307A mutation by DNA sequencing, the 3,826-bp BamHI–PshAI fragment was transferred into pST76K-SR. Finally, to prepare a shuttle vector for incorporation of a FLAG-tagged wt *vLIP* into the pRB-1B BAC, the pEco4.268\_*vLIP*\* plasmid was opened with BamHI and PshAI, and the 3,850-bp fragment was transferred to pST76K-SR (Fig. 5).

**Shuttle mutagenesis and BAC DNA preparation.** The pST76K-SR plasmid (a gift of Martin Messerle), which has been previously described (1, 11), contains a temperature-sensitive origin of replication, as well as genes encoding the bacterial recombinase RecA, the negative selection marker SacB, and kanamycin resistance. The pST76K-SR shuttle constructs described above were electroporated into DH10B *E. coli* harboring the pRB-1B BAC, plated on Luria Bertani (LB) agar plates containing kanamycin (50 µg/ml) and chloramphenicol (30 µg/ml), and incubated at 42°C. For the construction of a *vLIP* deletion mutant, miniprepations of BAC DNA from cointegrates were prepared from overnight cultures grown at 42°C, and DNA was analyzed by restriction enzyme analysis to verify cointegration of the shuttle construct. Verified cointegrates were then grown in LB broth at 37°C for 6 h in the presence of chloramphenicol but without kanamycin, so as to allow for the loss of the shuttle vector through a second RecA-mediated homologous recombination. Cultures were then streaked out on LB chloramphenicol plates containing 10% (vol/vol) sucrose to allow for negative selection by SacB. Colonies on these plates were then replica plated on kanamycin and chloramphenicol plates. Colonies that grew only on the chloramphenicol plates were screened by PCR for the presence of the deletion and

then were verified by restriction enzyme analysis. To repair the *vLIP* deletion mutant, pST76K-SR shuttle vectors bearing the wt *vLIP* or the FLAG-tagged version were electroporated into DH10B *E. coli* harboring the pRB-1B *vLIP*ΔMluI–Spell BAC. Shuttle mutagenesis was performed as described above, with the exception that the PCR screening procedures were adjusted accordingly. Large-scale purification of BAC DNA was performed using a QIAGEN Maxi-prep kit, as per the manufacturer's instructions for purification of very low copy number plasmids and cosmids.

**Baculovirus expression and protein purification.** Recombinant plasmid pBAC11-*vLIP* WT or pBAC11-*vLIP* S307A was cotransfected with BacVector3000 DNA into Sf9 insect cells using reagents from the BacVector kit (Novagen). Recombinant viruses were plaque purified twice and verified for expression by Western blotting with antibodies against *vLIP*.

For the purification of polyhistidine-tagged *vLIP* from supernatants of baculovirus-infected *T. ni* insect cells (multiplicity of infection, 1.0), TALON resin (Clontech, La Jolla, CA) was used. Briefly, supernatants were adjusted to a final concentration of 50 mM sodium phosphate (pH 7.0), 300 mM NaCl, 5 mM imidazole, and 10% glycerol and were mixed gently on a magnetic stirrer with pre-equilibrated TALON resin (Clontech, La Jolla, CA) for 20 min. The TALON beads were then spun down at  $700 \times g$ , washed twice with 20 volumes of TALON phosphate buffer, loaded onto a 10-ml TALON column, and washed with 5 volumes of TALON phosphate buffer. Recombinant proteins were eluted with TALON elution buffer containing 150 mM imidazole and dialyzed against HEPES-buffered saline overnight at 4°C to remove imidazole.

**Immunoprecipitation and Western blot analysis.** Protein concentrations were measured using the bicinchoninic acid reagent (Pierce Biotechnology Inc., Rockford, IL). Routinely, *vLIP* proteins were analyzed by SDS–8% polyacrylamide gel electrophoresis (PAGE), run in a Miniprotein III device (Bio-Rad Laboratories Inc., Hercules CA). For Western blotting, resolved proteins were transferred to Immobilon-P polyvinylidene difluoride (PVDF) membranes (Millipore, Billerica, MA) using a Bio-Rad semidry transfer apparatus. PVDF membranes were blocked using 5% powdered milk in  $1 \times$  Tris-buffered saline–Tween 20 (5% PM-TBST). Affinity-purified polyclonal rabbit antibodies raised against the peptide TKTTNENGHEKDSKD (amino acids 108 to 122 of *vLIP*) were used at a 1:1,000 dilution in 5% PM-TBST. The anti-FLAG antibody M2 (Stratagene) was purchased to detect epitope-tagged *vLIP* expressed from chicken cells. Horseradish peroxidase-conjugated donkey anti-rabbit immunoglobulin G (Amersham Biosciences) was employed as a secondary antibody at a 1:2,000 dilution in 5% PM-TBST, and horseradish peroxidase-conjugated goat anti-mouse immunoglobulin G (Jackson ImmunoResearch Laboratories, Inc., West Grove, PA) was used at 1:5,000 in 5% PM-TBST. ECL (Amersham Biosciences) chemiluminescent detection reagents were used according to the manufacturer's instructions to image bound secondary antibodies, and blots were exposed to BioMax MR film (Kodak). Digitized images were processed with Adobe Photoshop 7.0 software for Macintosh.

Immunoprecipitations were carried out overnight at 4°C in the presence of Complete Mini protease inhibitor (Roche) using 15 ml of cell culture supernatants of either pRB-1B- or pRB-1B-*vLIP*\*-infected CEL. Debris was removed by centrifugation at  $3,000 \times g$  for 10 min, and 40 µl of EZview ANTI-FLAG M2 affinity gel (Sigma-Aldrich) was added. Beads were washed three times in TBST and eluted by incubation with  $3 \times$  FLAG peptide (Sigma-Aldrich) as per the manufacturer's instructions. Concentration of cell culture supernatants for Western blot analysis was achieved using 20-kDa MWCO iCON devices (Pierce).

For deglycosylation reactions, peptide *N*-glycosidase F enzyme (PNGase F) (NEB) was used according to the manufacturer's instructions. Briefly, purified *vLIP* protein was incubated first for 10 min at 100°C in  $1 \times$  denaturation buffer (NEB) and then in the presence of PNGase F enzyme for 1 h at 37°C in  $1 \times$  G7 buffer (NEB) containing NP-40.

**Phospholipase assays.** Phospholipase assays on [ $^{14}$ C]dioleoylphosphatidylcholine ([1,2- $^{14}$ C]oleate) (New England Nuclear, Boston, MA) were performed as follows. Unlabeled dioleoylphosphatidylcholine (160 µg; Avanti Polar Lipids, Alabaster, AL) was combined with 40 µg of unlabeled phosphatidic acid and 5 µCi of [ $^{14}$ C]dioleoylphosphatidylcholine, and organic storage solvents were dried off under a stream of  $N_2$ . Four hundred microliters of lipase assay buffer (100 mM Tris-HCl, pH 8.0, 150 mM NaCl, 2 mM  $CaCl_2$ ) was added to the dry lipid film. Lipids were sonicated, and 40 µl of lipid micelles was transferred to microcentrifuge tubes on ice. Assays were initiated by adding 10 µl containing 10 ng of either recombinant purified wt *vLIP* protein, S307A *vLIP* protein, or chicken K60 chemokine (baculovirus expressed) as a negative control to the 40 µl of assay solution. Bee venom phospholipase  $A_2$  (Sigma-Aldrich) (10 ng) was used as a positive control. Reaction mixtures were incubated at 37°C for 1 h, and reactions were stopped by the addition of 187.5 µl of MeOH:CHCl<sub>3</sub> (3:1). Then 62.5 µl of 0.5 M HCl and 62.5 µl of CHCl<sub>3</sub> were added, and reaction products

were vortexed. Centrifugation at  $2,300 \times g$  was applied to separate phases, and 100  $\mu$ l of the organic phase was removed, dried under a stream of  $N_2$ , and resuspended in 10  $\mu$ l of developing solvent (90:10:10,  $CHCl_3$ :MeOH: $CH_3COOH$ ) (8). Lipids were then loaded onto activated silica gel 60A TLC plates (Sigma-Aldrich) and developed in a pre-equilibrated TLC chamber at room temperature. After the solvent front reached within 1.5 cm of the top of the plate, the plate was removed, allowed to air dry, and then exposed to BioMax MR film (Kodak).

**Triacylglycerol lipase assays.** Lipase assays on the radiolabeled triacylglyceride substrate [ $^3H$ ]triolein were performed essentially as described for the measurement of lipoprotein lipase activity by following the protocol of Briquet-Laugier et al. (16) using 12.8  $\mu$ Ci of freshly purified glycerol tri[9,10(n)- $^3H$ ]oleate (Amersham). Radioactive lipid was mixed with 75  $\mu$ l of a 200-mg/ml solution of cold triolein (Nu-Chek-Prep, Inc. Elysian, MN) and 10  $\mu$ l of a 100-mg/ml solution of lecithin, and the mixture was dried under a stream of  $N_2$ . Then 2.2 ml of 0.2 M Tris-Cl, pH 8.0, and 0.1 ml of 10% Pentex bovine serum albumin (Serologicals, Norcross, GA) were added to the dry lipid film and sonicated. Then 0.45 ml of 10% bovine serum albumin and 0.25 ml of heat-inactivated rat serum (a source of apolipoprotein-CII) were added to the substrate and mixed. Assays were performed in silica glass test tubes (Fisher Scientific, Pittsburgh, PA) and were initiated by adding recombinant protein to 100  $\mu$ l of the substrate. Samples were incubated for 60 min at 37°C, and reactions were stopped by the addition of 3.25 ml of MeOH: $CHCl_3$ :heptane (1.41:1.25:1, vol/vol/vol). Liberated fatty acids were extracted into the aqueous phase by the addition of 1 ml of 0.1 M potassium carbonate-borate buffer (pH 10.5) followed by vigorous vortexing for 15 seconds. The tubes were then centrifuged at  $500 \times g$  for 10 min at room temperature to separate the organic and aqueous phases. Finally, 1 ml of the aqueous phase was removed from each tube, mixed with 10 ml of scintillation fluid, and measured for radioactive counts in a scintillation counter.

**Animal experiments.** Specific-pathogen-free  $P_{20}$  line chickens (1 day old) were infected by intramuscular injection with 1,000 PFU of various viruses. Mock-infected birds received intramuscular injection of uninfected CEC in culture medium supplemented with 10% FBS. Experiment 1 included five groups of 15 birds infected with viruses reconstituted from pRB-1B, as well as an additional mock-infected group. The specific viruses tested were parental pRB-1B, pRB-1B *vLIP*-rev (*vLIP*-rev), pRB-1B *vLIP*<sup>\*</sup>-rev (*vLIP*<sup>\*</sup>-rev), pRB-1B *vLIP* $\Delta$ MluI-SpeI ( $\Delta$ *vLIP*), and pRB-1B-*vLIP* S307A (*vLIP* S307A). Experiments 2 and 3 included *vLIP*<sup>\*</sup>-rev,  $\Delta$ *vLIP*, and *vLIP* S307A. In experiment 2, 8 birds per group were infected, and in experiment 3, 10 birds per group were used. Experiments were allowed to proceed for 8 weeks, after which all surviving birds were sacrificed and necropsies were performed in a randomized, blind manner. Birds that died within the first week of the experiments were excluded from the studies. During the course of the experiments, birds that presented with Marek's disease symptoms were sacrificed, and necropsies were performed. Tumor incidence, morbidity, and mortality were recorded. In the third experiment, blood samples were obtained from all birds at days 4, 12, 15, and 19 postinfection (p.i.) by wing vein puncture. Data were analyzed using the SAS package for Windows, v8.2 (SAS Institute, Cary, NC), using the chi-square and Fisher's exact tests.

**Real-time qPCR.** Real-time quantitative PCR (qPCR) was performed on an ABI PRISM 7700 Sequence Detector (Applied Biosystems), and data were analyzed using ABI PRISM SDS 1.9.1 software on a Macintosh computer. For all reactions, TaqMan Universal PCR Master Mix, No AmpErase UNG (Applied Biosystems), was used. Reactions were run in MicroAmp 96-well plates (Applied Biosystems) in a final volume of 25  $\mu$ l per reaction. Reaction conditions were 50°C for 2 min, 95°C for 10 min, followed by 40 cycles of 15 s at 95°C and 1 min at 60°C. Samples were measured in duplicate on DNA samples obtained from 10  $\mu$ l of whole chicken blood. DNA was prepared using the QIAGEN DNeasy tissue kit using a final elution volume of 400  $\mu$ l, and 5  $\mu$ l was used in each qPCR. The qPCR probes and primer sets used in this study were configured to detect the MDV-1 *gD* gene or the chicken genomic inducible nitric oxide synthase (*iNOS*) gene exactly as described previously (Table 1) (36, 43). Probes for detection of *gD* and *iNOS* were labeled with 6-carboxyfluorescein (FAM) as the reporter and with Black Hole Quencher-1 (BHQ1) as the quencher dye (Eurogentec N.A., San Diego, CA). The primer pairs used were ck-*iNOS* F-ck-*iNOS* R and *gD* F-*gD* R (Table 1).

Standards of known copy numbers were run in triplicate to generate a standard curve for each qPCR and consisted of a  $\log_{10}$  serial dilution ranging from  $5 \times 10^6$  to  $5 \times 10^1$  copies in the case of the ck-*iNOS* target plasmid and from  $5 \times 10^6$  to  $5 \times 10^0$  copies in the case of MDV *gD*. The plasmid target used for generation of a standard curve for quantitation of chicken DNA copies in the unknown samples was plasmid pBS-*iNOS*, which harbors cDNA of the chicken *iNOS* gene (obtained from Keith Jarosinski) (50). The target DNA used for the generation of the *gD* standard curve was the MDV BAC20 clone (72). Probes were used at

a final concentration of 250 nM, and primers were used at a final concentration of 900 nM. Threshold cycle number values ( $C_T$ ) were calculated to correspond to the upper 10-fold standard deviation of the background fluorescence signal.

## RESULTS

**Characterization of the *vLIP* transcript.** The *vLIP* ORF had been identified in close proximity to the terminal repeat long ( $TR_L$ ) region in the  $U_L$  region of the MDV genome (Fig. 1a). The lymphoblastoid MSB-1 cell line was used as a source of RNA samples for cDNA cloning and Northern blot analysis. A cDNA of the *vLIP* transcript spanning the first coding sequences to the poly(A) site was obtained by RT-PCR on RNA from sodium butyrate-induced MSB-1 cells. In contrast, *vLIP* could not be amplified from RNA samples derived from non-induced cells, indicating that *vLIP* is not transcribed during latency, and Northern blot analysis confirmed such an assertion (see below). Comparison of the *vLIP* cDNA to the corresponding genomic DNA sequence, shown in Fig. 1a, revealed that a 70-bp intron was removed from the *vLIP* transcript by splicing, which brings sequences encoding the signal peptide in frame with the rest of the *vLIP* ORF.

In order to characterize the size and kinetic class of the *vLIP* transcript, RNAs from MSB-1 cells induced with butyrate were collected after treatment for 30 h with PFA, an inhibitor of viral DNA polymerase. A  $^{32}P$ -labeled riboprobe antisense to a 376-bp region of the *vLIP* reading frame, corresponding to *vLIP* amino acids 476 to 601, resulted in the detection of a single sodium butyrate-inducible, foscarnet-sensitive transcript of  $\sim 2.4$  kb (Fig. 1b). RNA integrity was monitored by UV imaging of ethidium bromide-stained RNAs, both prior to and after capillary transfer; levels of intact rRNA were comparable across all samples (Fig. 1b). From the above experiments we concluded that the MDV *vLIP* ORF is 2,271 bp in length and is expressed with late kinetics from one major spliced mRNA transcript of 2.4 kb.

**Analysis of *vLIP* amino acid similarity to cellular lipases.** As a first approach to elucidate the function of the protein encoded by *vLIP*, comprehensive structural predictions were performed. The homology between *vLIP* and cellular lipases is especially significant in that structural residues essential to lipase activity are—for the most part—well conserved in the viral protein. Figure 2a depicts an amino acid sequence alignment of *vLIP* against homologous residues from a wasp venom phospholipase and the human lipoprotein lipase. A secondary-structure prediction for *vLIP*, generated by GenTHREADER analysis (45), is also included in Fig. 2a to demonstrate the placement of catalytic-triad positions in relation to conserved secondary-structure elements found among pancreatic lipases. The oxyanion hole residues, Phe/Trp 77 and Leu153 (by HPL numbering), which serve to stabilize tetrahedral reaction intermediates during enzyme activity, are conserved in *vLIP* and its adenovirus homologues. The serine residue at position 307 of *vLIP* (HPL numbering 152), representing the triad nucleophile (15, 79, 81), is also well conserved and is found in a typical HPL-like GHSLG motif.

In contrast, the aspartic acid position of the catalytic triad, located at position 335 on the *vLIP* chain (HPL numbering 176), bears an asparagine substitution in each of the MDV strains for which sequence data are available (Fig. 2a) (49, 78).

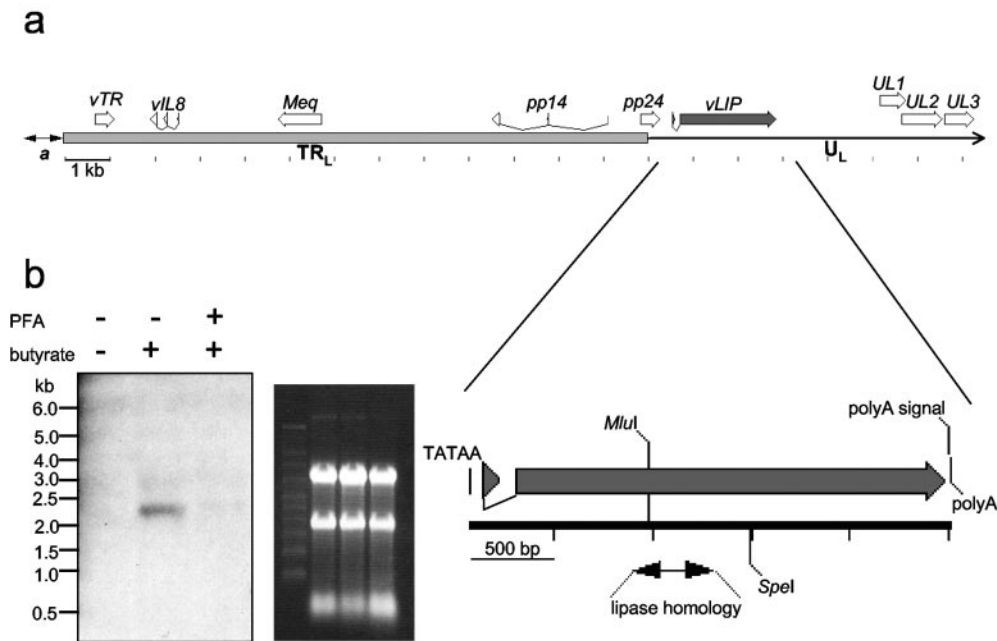


FIG. 1. (a) Location of *vLIP* relative to other genes in the MDV genome. The *vLIP* open reading frame is drawn to scale; a bar representing 1 kb is drawn and labeled. The terminal repeat long ( $TR_L$ ) region, the  $U_L$  region, and an  $a$ -like sequence (double-headed arrow) are also indicated. Several MDV-1-specific ORFs neighboring the *vLIP* gene are displayed, as are the conserved genes  $U_L1$  to  $U_L3$ . The gene organization of the *vLIP* transcript is shown in more detail below, also drawn to scale. A 500-bp bar is shown, and the TATA box, putatively used to initiate *vLIP* transcripts, as well as the poly(A) site and poly(A) signal, is labeled. *MluI* and *SpeI* restriction sites flanking the lipase homology region, indicated by a double-headed arrow, are also labeled. (b) The *vLIP* transcript as visualized by Northern blotting. In the left panel, a Northern blot was probed with a single-stranded riboprobe antisense to *vLIP* mRNA. RNA samples were derived from MSB-1 tumor cells which had been either treated for 24 h in the presence of sodium butyrate to induce virus replication or left untreated, as indicated. PFA was also used where indicated, to show the sensitivity of *vLIP* transcription to inhibition of DNA replication. To the right, RNA samples used in Northern blotting were separated on denatured agarose gels, stained with ethidium bromide, and imaged to verify that RNA integrity and quantity were comparable across all samples tested. An RNA marker (Ambion) was included to determine molecular weights.

The equivalent HPL mutation, D176N, has been shown to lead to a loss of enzyme activity in HPL (52). Furthermore, sequence homology of *vLIP* to cellular lipases is much lower in the region of the catalytic-triad histidine residue (Fig. 2b). In this region, pancreatic lipases conserve a “lid” or “flap” domain, which is delimited by a pair of cysteine residues that form the structure by participating in a disulfide bond (21, 81, 82). In some lipases, the lid regulates access to the enzyme active site and accounts for an observed preference for water-insoluble substrates known as “interfacial activation” (44). The triad histidine residue is normally located 2 amino acid positions downstream of the second cysteine residue of the pair that forms the lid. While a pair of cysteines and a histidine are present in the alignment of *vLIP* with relevant cellular lipases, the second cysteine involved in lid formation does not align favorably and the putative triad histidine residue would be positioned on the “lid,” instead of just after it (Fig. 2b). Thus, based on the structural criteria, it is not clear a priori whether MDV *vLIP* would behave like a prototypic (or conventional) lipase.

**MDV *vLIP* lacks lipase activity.** Lipoprotein lipases are a subset of the pancreatic lipase gene family; thus, the asparagine substitution observed in *vLIP* at the acid position (D335N [Fig. 2a]) would most likely render the protein incapable of lipase activity (52). To eliminate the possibility that *vLIP* is a functional lipase enzyme whose triad acid residue has been

shifted from the preferred location in strand  $\beta 6$  to a position following strand  $\beta 7$  (71), functional assays were performed to demonstrate or exclude enzymatic activity.

In order to obtain significant amounts of recombinant protein, wt *vLIP* and the *vLIP* serine nucleophile site mutant S307A, which would be unable to make nucleophilic attacks on lipid substrates, were purified from insect cell culture supernatants. A Coomassie-stained SDS-PAGE gel and Western blot analysis of the steps performed during the purification of the recombinant proteins are shown in Fig. 3a. Highly purified recombinant *vLIP* protein was tested on  $^{14}\text{C}$ -labeled phospholipid and  $^3\text{H}$ -labeled triacylglyceride substrates *in vitro*. Experiments were repeated several times, and representative results are shown as thin-layer chromatography demonstrating separation of substrate and reaction products for a phospholipid substrate, 1,2-dioleoylphosphatidylcholine ([1,2- $^{14}\text{C}$ ]oleate), in which each fatty acid chain is radiolabeled (Fig. 3b) and as a phase separation-based assay for the triacylglyceride substrate glycerol tri[9,10(n)- $^3\text{H}$ ]oleate (triolein) (Fig. 3c). In each reaction, 10 ng of insect cell-derived recombinant *vLIP* was used. Recombinant wt *vLIP* did not yield activity on phospholipid substrates above background levels observed in buffer alone, with a nonspecific protein control (K60), or with the S307A *vLIP* mutant (Fig. 3b). In contrast, phospholipid hydrolysis could readily be observed in samples to which 10 ng of bee venom phospholipase was added (Fig. 3b). As shown in Fig. 3c,

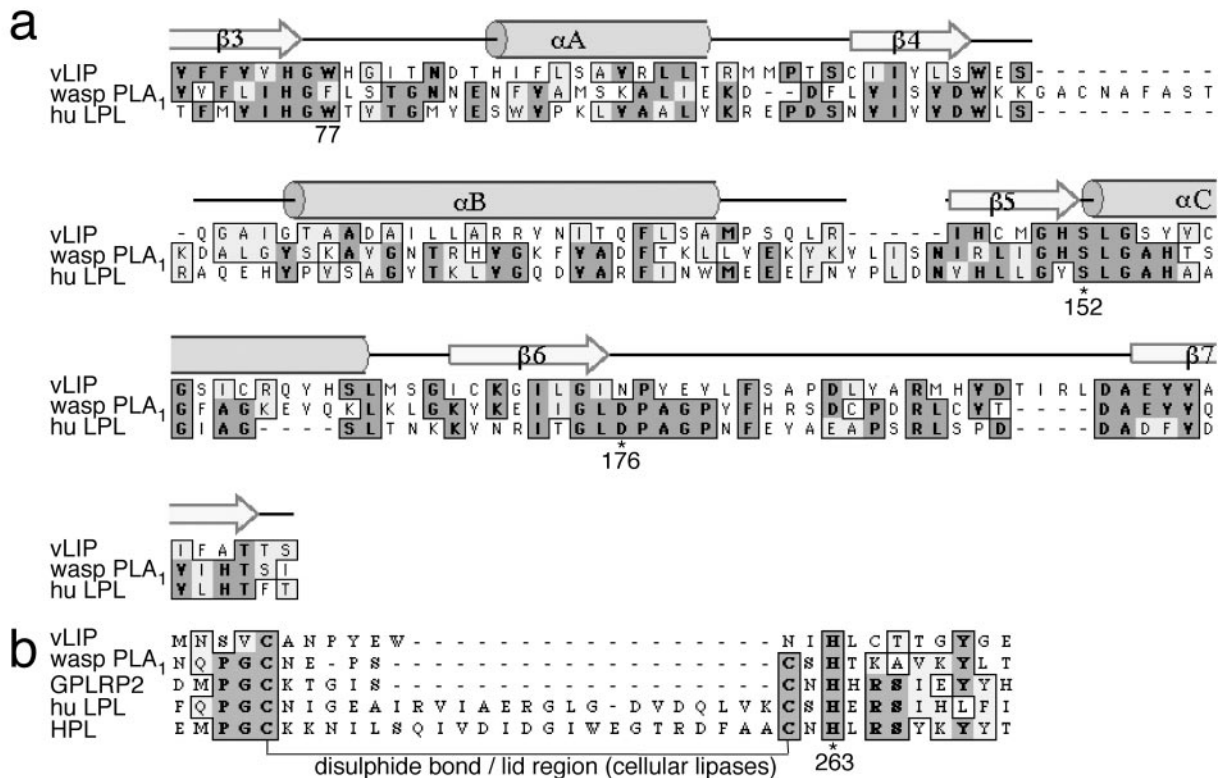


FIG. 2. (a) vLIP shows significant amino acid similarity to the  $\alpha/\beta$  hydrolase fold of pancreatic lipases. Amino acids 229 to 369 of MDV vLIP are aligned against homologous regions of a wasp venom phospholipase A<sub>1</sub> (wasp PLA<sub>1</sub>; *Polistes annularis*; GenBank accession no. Q9U6W0) and the human lipoprotein lipase (hu LPL; GenBank P06858). A secondary-structure prediction for vLIP, generated by GenTHREADER, is displayed above the alignment: arrows represent  $\beta$ -strands, round columns represent  $\alpha$ -helices, and coil regions are represented by a black line. Catalytic-triad nucleophile and acid positions are indicated with asterisks and numbered according to HPL conventions. Additionally, an oxyanion hole residue (Phe/Trp 77) is also numbered by HPL conventions. The other oxyanion hole residue is located at position 153, immediately following the serine nucleophile found at position 152. (b) vLIP does not align favorably with the lid region cellular lipases. vLIP amino acid positions 391 to 412 are shown aligned against lid regions of the following pancreatic lipases: wasp PLA<sub>1</sub> (*P. annularis*), guinea pig PLRP2 (GPLRP2; UID 1942400), hu LPL, and HPL (GenBank P16233). Cysteines known to be involved in disulfide bonds to form the respective lid regions are indicated, and the catalytic-triad histidine position is asterisked and numbered according to HPL conventions. The putative triad histidine residue of vLIP does not appear appropriately configured relative to important cysteines involved in disulfide bonding in relevant cellular lipases.

vLIP did not exhibit hydrolytic activity on a triacylglyceride substrate above background levels, either. From the results of the (phospho)lipase assays, we concluded that vLIP, consistent with the unfavorable D335N substitution, lacked detectable hydrolytic activity on (phospho)lipid substrates.

**The vLIP gene product is secreted and undergoes N glycosylation.** When vLIP cDNA was expressed in mammalian 293T cells (data not shown) or in chicken cells during virus replication (see below), the size of the mature, secreted protein was observed to be approximately 120 kDa, although the calculated molecular mass of vLIP (residues 31 to 756) is 81.8 kDa, taking into account signal peptide cleavage, which is predicted to remove the first 30 amino acids of the vLIP polypeptide (57, 58). To analyze putative vLIP glycosylation in more detail, vLIP was expressed in *T. ni* insect cells using a baculovirus expression system. SDS-PAGE, followed by Western blotting with a peptide-specific rabbit antibody, was used to compare the electrophoretic mobilities of purified vLIP protein before and after treatment with PNGase F. Untreated vLIP had an apparent molecular size of approximately 110 kDa, but treatment with PNGase F increased the electrophoretic mobility of

vLIP, and the apparent molecular size was reduced to approximately 76 kDa (Fig. 4). These findings clearly indicated that the discrepancy between the 81.8-kDa predicted size of the vLIP protein chain and the size observed when vLIP was expressed in eukaryotic cells can be accounted for by N glycosylation.

**Construction and in vitro characterization of vLIP MDV mutants.** The results obtained from the sequence analyses and the lipase assays suggested that vLIP may not serve as a conventional lipase enzyme. In addition, previous results had suggested that vLIP was not essential for viral replication in culture (39). In order to test whether the lipase homology of vLIP had any measurable role during in vivo replication of MDV, vLIP mutant MDVs were constructed from pathogenic strain RB-1B cloned as a BAC (pRB-1B) (64). As outlined in Fig. 5, by using shuttle mutagenesis techniques in *E. coli*, two vLIP mutants were prepared from pRB-1B: an S307A point mutant of the nucleophile site (vLIP S307A) and an in-frame deletion of 173 amino acids in the lipase homologous region, spanning positions 256 to 426 ( $\Delta$ vLIP). Native (vLIP-rev) and C-terminally FLAG epitope tagged (vLIP\*-rev) vLIP revertant clones

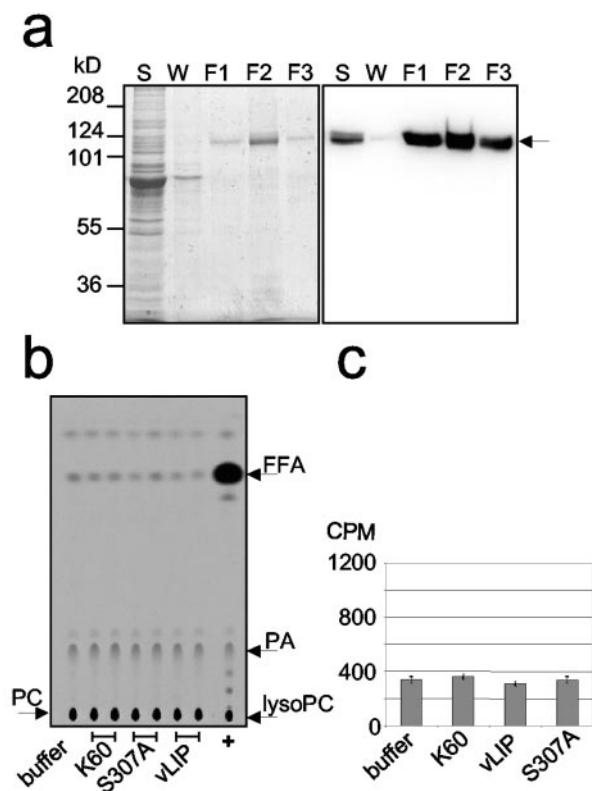


FIG. 3. (a) Purification of vLIP-6×His from a baculovirus expression system. Recombinant protein was expressed and purified. Proteins obtained from the various steps during metal affinity chromatography were separated by SDS-PAGE and stained with Coomassie blue (left panel). S, raw supernatant from baculovirus-infected *T. ni* cells; W, column wash; F1 to F3, fractions 1 through 3 after elution buffer was applied to the column. The right panel depicts results of Western blotting performed on an identical gel where vLIP is detected using a rabbit anti-vLIP polyclonal antibody preparation raised against a vLIP synthetic peptide. vLIP protein is indicated by an arrow. (b) vLIP shows no detectable activity on phospholipid or triacylglyceride substrates. A thin-layer chromatography-based phospholipase assay of recombinant vLIP protein on the  $^{14}\text{C}$ -labeled substrate 1,2-dioleoylphosphatidylcholine is shown, where 10 ng of each protein was used in each assay. Samples are indicated as follows: buffer, buffer alone; K60, baculovirus-expressed negative-control protein; S307A, vLIP S307A serine nucleophile mutant; vLIP, wt vLIP; +, positive control (bee venom phospholipase  $\text{A}_2$ ). Except for the buffer and the positive control, all samples were tested in duplicate, as indicated by bracketed bars. Free fatty acid released by hydrolysis (FFA), phosphatidylcholine (PC), phosphatidic acid (PA), and lysophosphatidylcholine (lysoPC) are each indicated by an arrow. (c) Results of a phase separation-based assay on  $^3\text{H}$ -labeled glycerol trioleate are shown as a bar graph of counts per minute (CPM) of water-soluble  $^3\text{H}$ -labeled free oleic acid released from the  $^3\text{H}$ -labeled substrate during the assay, with error bars indicating standard deviations of triplicate measurements. Ten nanograms of each protein sample was used per assay. Label abbreviations are as indicated above for the phospholipase assay.

were prepared from the  $\Delta\text{vLIP}$  mutant BAC, also by shuttle mutagenesis in *E. coli* (Fig. 5).

The DNA of each pRB-1B mutant was analyzed by several restriction enzymes in order to confirm that the appropriate changes were present and that no spurious rearrangements took place during shuttle mutagenesis. The results of an EcoRI

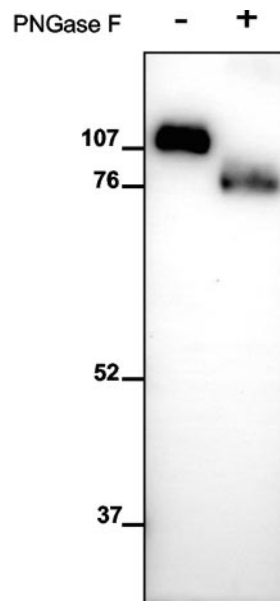


FIG. 4. Western blot analysis of vLIP after treatment with PNGase F. A sample of baculovirus-expressed and purified vLIP was treated for 1 h in the presence or absence of PNGase F. Then samples were separated by 8% SDS-PAGE, transferred to a PVDF membrane, and detected using a vLIP-specific rabbit antibody. Treatment of vLIP with an endoglycosidase, PNGase F, resulted in a significant increase in electrophoretic mobility, and the apparent molecular size of vLIP was reduced from 110 kDa to approximately 76 kDa. A molecular weight marker (Bio-Rad) was used as a size standard.

digest are shown in Fig. 6a, where the DNA fragment encoding the vLIP gene migrated at 3.743 kb in the digest of the  $\Delta\text{vLIP}$  mutant owing to the loss of 519 bp, instead of the usual 4.262 kb observed in the digests of parental pRB-1B or vLIP-rev. The vLIP\*-rev mutant exhibited a slight decrease in mobility in the fragment encoding vLIP, causing it to run as a doublet with the next largest band in the digest, which is 4.524 kb (Fig. 6a). This shift reflects the incorporation of an additional 24 bp of sequence encoding the 8-amino-acid FLAG epitope. DNA sequencing of a 4-kbp region of each mutant and revertant BAC was performed to further confirm the genetic makeup of the vLIP region of each mutant BAC; it demonstrated that only the intended modifications were introduced (data not shown).

Virus was recovered from BAC DNA after transfection of CEC, and growth kinetics demonstrated that there were no significant defects in virus replication of either vLIP mutant in vitro (Fig. 6c). To confirm that a FLAG-tagged vLIP was indeed expressed in virus-infected cells, the FLAG epitope-tagged revertant, vLIP\*-rev, was grown on CEC, and supernatants and cell lysates were compared to those from parental pRB-1B virus. Anti-FLAG immunoprecipitation, as visualized by Western blotting using both anti-FLAG antibody and the vLIP-specific rabbit polyclonal antibody, clearly demonstrated a distinct band of approximately 120 kDa specific to vLIP\*-rev supernatants (Fig. 6b). However, vLIP was not detected in infected-cell lysates or in concentrated supernatants by either antibody. The latter result suggested that, consistent with the presence of a suboptimal cytosine at +4 in the Kozak sequence

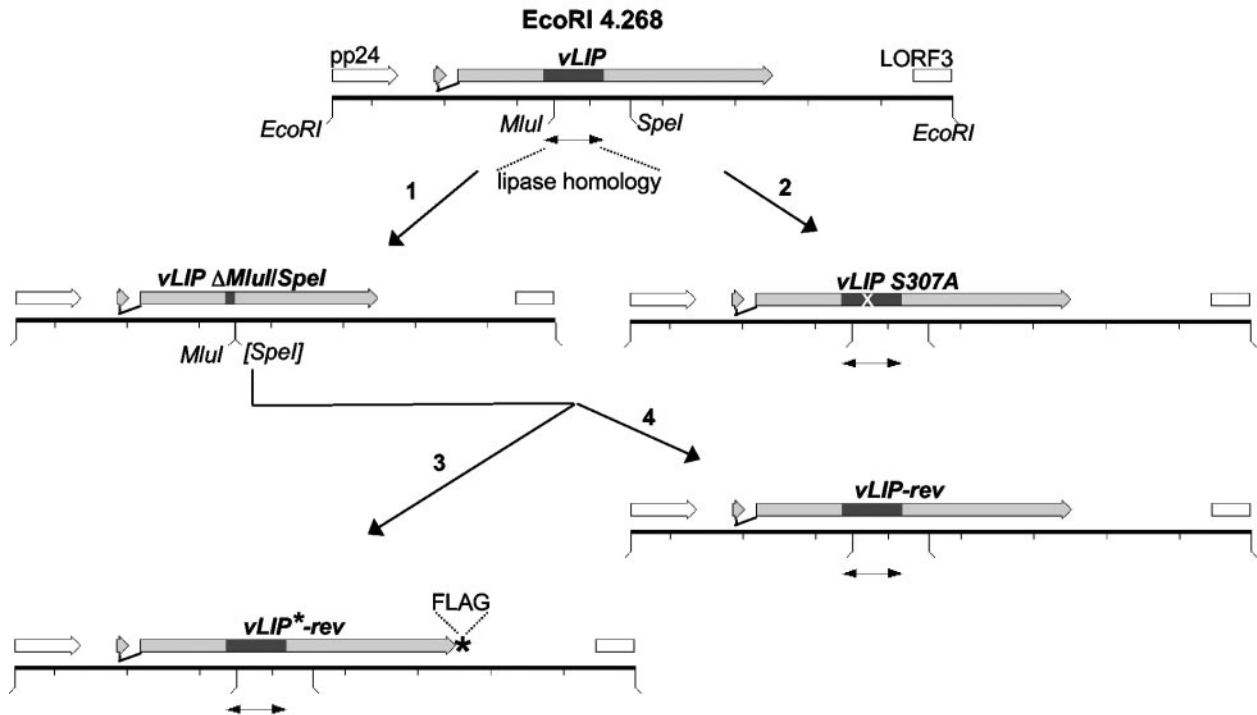


FIG. 5. Shuttle mutagenesis strategy used to construct *vLIP* mutant MDVs and revertants in the pRB-1B BAC. A 4.268-kb fragment of the Md5 strain of MDV, containing the *vLIP* gene and portions of neighboring genes, was cloned into pST76K-SR, a RecA-based shuttle vector. In step 1 (labeled arrow), an in-frame deletion of *vLIP* amino acids 256 to 426 was incorporated into the pRB-1B BAC by shuttle mutagenesis using a pST76K-SR-based shuttle vector bearing the same deletion ( $\Delta$ MluI-SpeI), yielding  $\Delta$ *vLIP*. In parallel (step 2), an alanine point mutant of the *vLIP* serine nucleophile position (*vLIP* S307A) was incorporated into pRB-1B. As depicted in steps 3 and 4, shuttle mutagenesis was performed on the  $\Delta$ *vLIP* BAC to generate C-terminally FLAG tagged *vLIP* (*vLIP*\*-rev) and native *vLIP* (*vLIP*-rev) revertants. Relevant features of the DNA fragment used and modified in shuttle mutagenesis procedures are labeled accordingly. A double-headed arrow represents lipase homology in the *vLIP* ORF, a white X represents the location of the S307A change, a FLAG epitope tag is represented as a labeled asterisk, and the MluI and SpeI sites which were used to remove the lipase homology region of *vLIP* are labeled accordingly.

at the translation initiation site of *vLIP* (ACAATGC), *vLIP* is not highly expressed during MDV replication in cultured cells (47–49, 78). From these results we concluded that *vLIP* was secreted upon lytic infection of chicken cells and that deletion or mutation of *vLIP* sequences did not have a detrimental effect on MDV growth properties in vitro.

***vLIP* is a determinant of virulence.** In a preliminary experiment, each of the mutant and revertant viruses was used to infect a group of 15 chickens of the susceptible P<sub>2a</sub> line. Mock-infected birds and animals infected with parental virus reconstituted from pRB-1B were used as negative and positive controls, respectively. In this first experiment, increased survival and reduced incidence of Marek's disease, characterized by wasting, visceral tumors, and paralysis, were observed in the *vLIP* mutant virus groups relative to those groups infected with the parental or revertant virus (Tables 2 and 3). Because the observed differences in mortality in the first experiment amounted only to about a 30% reduction from the levels observed for parental and revertant viruses, two further animal studies were conducted to confirm the observed effects. In order to minimize the number of experimental animals, the pRB-1B and the untagged *vLIP* revertant (*vLIP*-rev) group were not included in any further experiments. The reduction in the number of experimental animals was possible because the first trial had demonstrated that the parental pRB-1B, the

FLAG-tagged revertant *vLIP*\*-rev, and the native *vLIP* revertant *vLIP*-rev were equally virulent, inducing characteristic gross T-cell lymphoma at rates greater than 90% (Table 2). Therefore, the notion that the incorporation of a FLAG epitope-tag at the C terminus of the *vLIP* reading frame might abrogate pathogenesis in vivo was no longer a concern.

The results of the second and third experiments suggested that the reduction in virulence observed in the first study was a repeatable phenotype for both the *vLIP* deletion and nucleophile mutant viruses. In Table 2, the observed defect of *vLIP* mutant viruses in causing Marek's disease is summarized, as measured by incidence of gross lymphoma in visceral organs or musculature at necropsy. In the course of the three experiments, the *vLIP*\*-rev revertant virus was observed to cause gross lymphoma at rates of 92 to 100%, but  $\Delta$ *vLIP* caused gross tumors in only 44 to 64% of birds, while the *vLIP* S307A point mutant virus caused tumors in 58 to 71% of birds. Statistical analyses using Fisher's exact and  $\chi^2$  tests demonstrated that the reductions in tumor incidence in both groups were statistically significant ( $P < 0.004$ ).

In order to elucidate whether any measurable defect in early lytic replication of *vLIP* mutant viruses could be identified, samples of whole blood were taken at days 4, 7, 12, 15, and 19 p.i. from every bird in the third experiment, which included 9 to 10 birds per group. Blood samples (10  $\mu$ l) were subjected

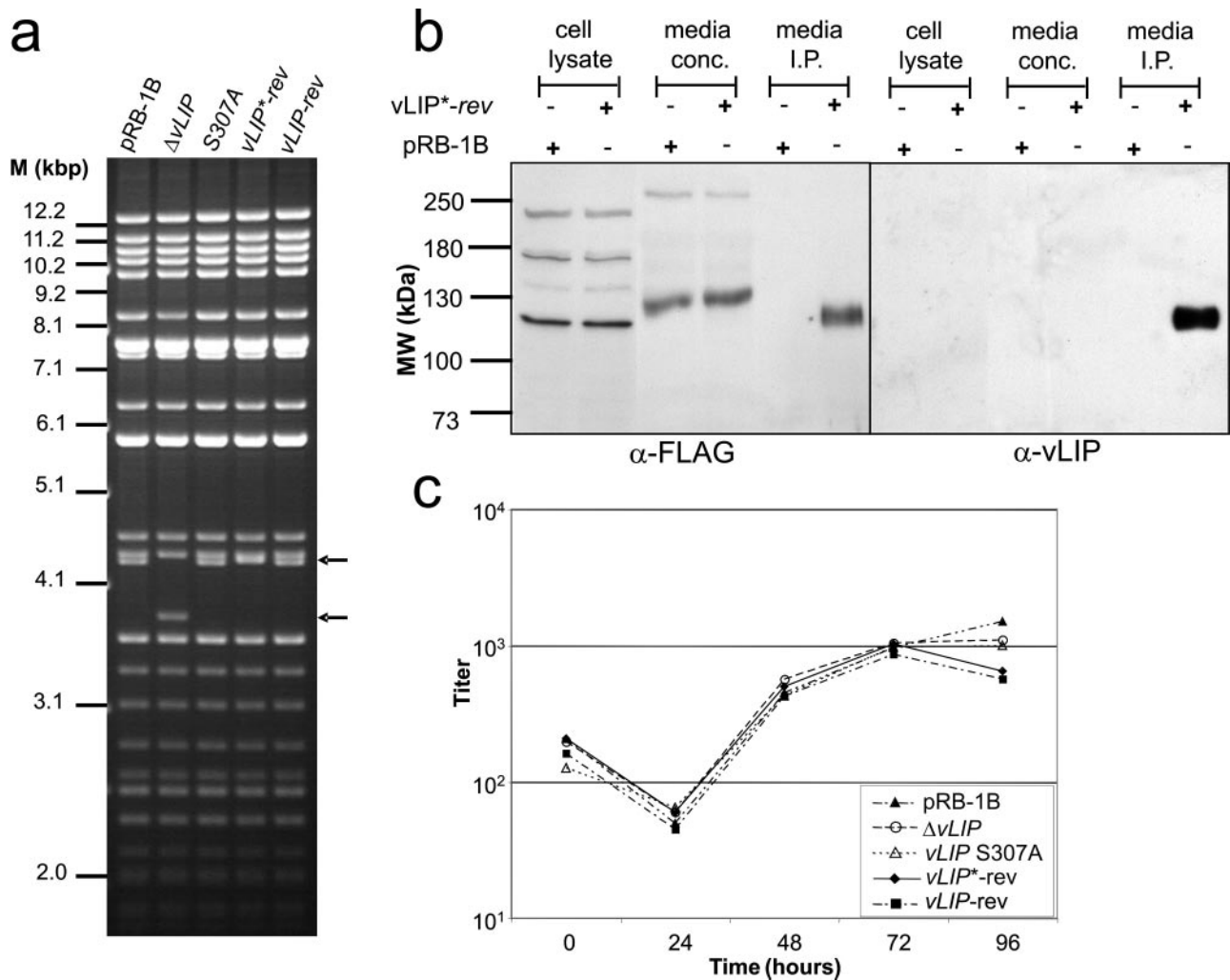


FIG. 6. (a) Agarose gel of an EcoRI restriction digest of each pRB-1B-based BAC used in the animal study. DNA was digested and separated on a 0.8% gel alongside a 1-kb DNA ladder (Invitrogen). The upper black arrow to the right of the gel indicates the fragment containing the *vLIP* gene, and the lower arrow indicates increased mobility of the *vLIP* fragment where a 519-bp  $\Delta$ MluI-SpeI deletion has been incorporated into the  $\Delta$ *vLIP* BAC by shuttle mutagenesis. (b) Immunoblot analysis of C-terminally FLAG tagged *vLIP* from *vLIP*\*-*rev*-infected CEC. Cell lysates, 7 $\times$ -concentrated supernatants, and proteins immunoprecipitated from supernatants of *vLIP*\*-*rev*- and parental pRB-1B-infected cells were separated by 6% SDS-PAGE, transferred to a PVDF membrane, and probed with anti-FLAG ( $\alpha$ -FLAG) antibody M2 (Stratagene) or with a *vLIP*-specific rabbit polyclonal antibody. A specific band exhibiting an  $M_r$  of approximately 120 kDa is seen in the *vLIP*\*-*rev* immunoprecipitate (I.P.) but is not detectable in cell lysates, supernatants, or an immunoprecipitate run in parallel on supernatants from parental pRB-1B-infected CEC. Prestained molecular weight ladders (MBI Fermentas and Bio-Rad) were used. The  $\alpha$ -FLAG blot was exposed for 3 min, and the  $\alpha$ -*vLIP* blot was exposed for 25 min. Nonspecific bands are seen only in the  $\alpha$ -FLAG blot. (c) Growth curves of MDV reconstituted from parental and mutant pRB-1B-based BAC clones as determined on CEC. Cells were infected with 200 PFU, and at the indicated times p.i., infected cells were trypsinized and coseeded with fresh CEC. Five days after coseeding, the number of virus plaques was recorded. All mutant viruses generated (see key in lower right corner) did not show significant differences in growth kinetics from parental pRB-1B.

to direct DNA purification, and aliquots of DNA, each equivalent to 0.125  $\mu$ l of whole blood, were analyzed by real-time PCR. This small quantity of DNA sample, though it included erythrocyte DNA, routinely was measured to contain  $7 \times 10^5$  to  $1.6 \times 10^6$  chicken genome copies, and copies detected per sample were consistent within each time point.

While virus DNA could not be detected in every sample collected on day 4 p.i., virus was reliably detected in all samples from day 7 and all later time points. The *in vivo* data on levels in blood shown in Fig. 7a indicate that, compared to chickens infected with revertant virus, *vLIP* mutant virus-infected chickens experienced reduced levels of viral DNA in peripheral

blood at late, but not early, time points during lytic virus infection. Average levels of virus DNA in peripheral blood appeared nearly indistinguishable between all three groups at days 7 and 12, but *vLIP*\*-*rev* showed two- to threefold-higher average levels of viral DNA at days 15 and 19 than the mutants, which remained indistinguishable from each other (Fig. 7a).

Notably, the trend seen in Fig. 7a is echoed in the survival curves in Fig. 7b, which shows the percent survival per week using the combined data from experiments 2 and 3. The revertant virus was observed to cause onset of Marek's disease more rapidly than the *vLIP* mutants, which each showed increased numbers of asymptomatic birds surviving the full 8

TABLE 2. Tumor incidence in chickens during in vivo studies of *vLIP* mutants

Virus genotype	Tumor incidence <sup>a</sup>				P value <sup>b</sup> (vs <i>vLIP</i> *- <i>rev</i> )
	Expt 1	Expt 2	Expt 3	Total	
<i>ΔvLIP</i> <sup>c</sup>	63.6 (7/11)	50 (4/8)	44.4 (4/9)	53.6 (15/28)	0.0004
<i>vLIP</i> S307A <sup>c</sup>	58.3 (7/12)	71.4 (5/7)	70 (7/10)	65.5 (19/29)	0.0036
<i>vLIP</i> *- <i>rev</i>	92.3 (12/13)	100 (6/6)	100 (9/9)	96.4 (27/28)	NA
<i>vLIP</i> - <i>rev</i>	93.3 (14/15)	NA	NA	93.3 (14/15)	1.000
pRB-1B	90.9 (10/11)	NA	NA	90.9 (10/11)	0.4924

<sup>a</sup> Expressed as the percentage of animals with tumors (number of animals with tumors/total number of animals). NA, not applicable.

<sup>b</sup> The  $\chi^2$  test was used to compare pooled data for *ΔvLIP* and *vLIP* S307A from experiments 1 to 3, to those for *vLIP*\*-*rev*.

<sup>c</sup> *ΔvLIP* and *vLIP* S307A were not significantly different from each other in tumor incidence ( $P = 0.3655$ ).

weeks to the end of the experiment (Fig. 7b). Although a subset of birds surviving to the end of the experiment invariably presented with characteristic Marek's disease tumors upon necropsy, over the three experiments the *vLIP* deletion and nucleophile substitution mutant groups each consistently contained a number of birds that survived to full term without any apparent Marek's disease pathogenesis at necropsy (Table 3). The percentages of birds surviving to full term without gross lymphoma or other MD symptoms at necropsy ranged from 20 to 29% for *vLIP* S307A and from 25 to 44% for *ΔvLIP*. In contrast, in the *vLIP*\*-*rev* and *vLIP*-*rev* groups, completely asymptomatic birds were never observed among the few that survived to full term, and the scarce examples of birds free of gross lymphoma ( $n = 2$ ) represented cases where birds were sacrificed prior to the end of the experiment because they had presented with severe paralytic symptoms. From the experiments summarized in Table 2, Table 3, and Fig. 7, we concluded that deletion of *vLIP* or mutation of the protein's serine nucleophile resulted in reduced lytic virus replication in vivo and significantly lower numbers of chickens that developed and/or succumbed to Marek's disease.

DISCUSSION

In this study, we have demonstrated that the MDV *vLIP* gene product is derived from a late transcript, is glycosylated

TABLE 3. Survival to end of experiment without symptoms at final necropsy

Virus genotype	% of animals surviving (no. surviving/total no.)				P value <sup>a</sup> (vs <i>vLIP</i> *- <i>rev</i> )
	Expt 1	Expt 2	Expt 3	Total	
<i>ΔvLIP</i> <sup>b</sup>	27.3 (3/11)	25.0 (2/8)	44.4 (4/9)	32.1 (9/28)	<0.0001
<i>vLIP</i> S307A <sup>b</sup>	25.0 (3/12)	28.6 (2/7)	20.0 (2/10)	24.1 (7/29)	0.0081
<i>vLIP</i> *- <i>rev</i>	0 (0/13)	0 (0/6)	0 (0/9)	0 (0/28)	NA <sup>c</sup>
<i>vLIP</i> - <i>rev</i>	0 (0/15)	NA	NA	0 (0/15)	0.8009
pRB-1B	9.1 (1/11)	NA	NA	9.1 (1/11)	0.8735

<sup>a</sup> The  $\chi^2$  test was used to compare pooled data for *ΔvLIP* and *vLIP* S307A from experiments 1 to 3 to those for *vLIP*\*-*rev*.

<sup>b</sup> *ΔvLIP* and *vLIP* S307A were not significantly different from each other in survival ( $P = 0.2411$ ).

<sup>c</sup> NA, not applicable.

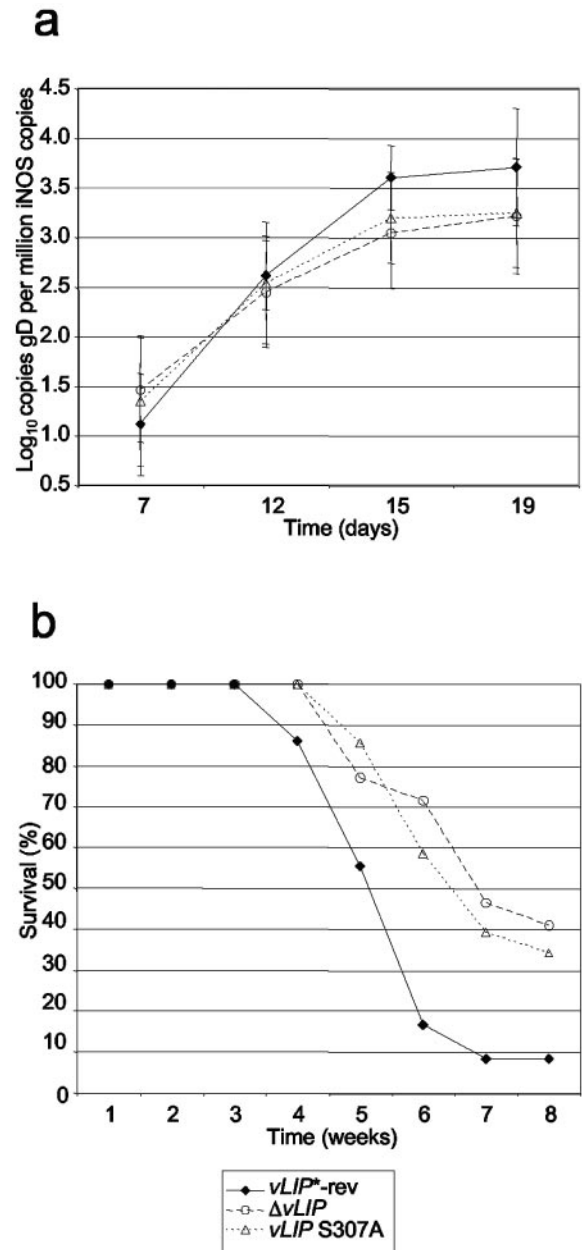


FIG. 7. (a) *ΔvLIP* and *vLIP* S307A show reduced lytic replication in vivo compared to revertant virus. Averaged data from real-time PCR analysis of a viral gene (gD) in total DNA from whole peripheral blood samples taken at 7, 12, 15, and 19 days p.i. are shown as copies of gD per 10<sup>6</sup> copies of a chicken gene (iNOS). (b) A survival curve following Marek's disease mortality shows that chickens infected with either the *ΔvLIP* or *vLIP* S307A virus, on average, survived at higher percentages and longer than those infected with a revertant virus (*vLIP*\*-*rev*).

and secreted, and is critical for maintaining the wild-type pathogenic potential of MDV.

The data obtained from the *vLIP* cDNA sequence indicated a postsplicing coding sequence of 2,271 bp with a poly(A) signal and a polyadenylation site located 12 and 25 bp from the termination codon, respectively. Taken together with the size of 2.4 kb visualized for the *vLIP* transcript during Northern

blot analysis, the data suggest that the TATA box present at -69 bp from the *vLIP* start codon is most likely used to initiate *vLIP* transcripts (Fig. 1a). The classification of *vLIP* as a fo-carnet-sensitive, late ( $\gamma$ ) transcript suggests that *vLIP* is coexpressed with other secreted viral factors implicated in immune modulation, such as *vIL-8* and glycoprotein C (31, 63). Therefore, *vLIP* is likely to be expressed as maturing virus particles are becoming ready for transfer to new host cells. Like *vIL-8*, another virally encoded soluble mediator which has been shown to be important for wild-type pathogenesis of MDV (26, 63), secreted *vLIP* may be involved either in the recruitment of new host cells or in the down-modulation of immune surveillance by cytotoxic T cells or NK cells.

Structural and lipase assay data present the first clues that *vLIP*, and at least some of its homologues in other avian herpesviruses and adenoviruses, may not behave as a conventional lipase enzyme *in vivo*. Lipases of the pancreatic lipase gene family employ  $\alpha/\beta$  hydrolase folds where the catalytic-triad acid residues are positioned immediately after the  $\beta 6$  strand and can be typically located in the context of a GLDP motif (Fig. 2a), but other  $\alpha/\beta$  hydrolase fold lipases position their acid residues following the  $\beta 7$  strand (71). PSI-BLAST and manual sequence analysis each suggest that *vLIP* is derived from the pancreatic lipase gene family, specifically from a lipoprotein lipase. Therefore, the presence of an uncharged (asparagine) instead of an acidic (aspartic acid) residue at the catalytic-triad acid position in *vLIP* argues strongly against the possibility that *vLIP* is a conventional lipase (Fig. 2a) (52), and this contention is indeed supported by negative lipase assays with recombinant *vLIP* (Fig. 3b and c). In addition, an N335D mutant was prepared, restoring the acid residue of the catalytic triad; however, this mutant also was negative in lipase assays (J. P. Kamil, unpublished data). Moreover, other sequence features of *vLIP* further substantiate the notion that *vLIP* is not a lipase. Besides poor homology in the lid region containing the triad histidine, two amino acid substitutions downstream of the acid residue, A178Y and P180V in reference to HPL, are similar to those (A178V and P180A) that have been experimentally demonstrated to account for the absence of lipase activity in PLRP1s (Fig. 2a) (10, 25, 67).

Based on negative lipase assays and an unfavorable substitution at the essential catalytic-triad acid position, we presently hypothesize that *vLIP* does not perform as a traditional lipase. Yet we have demonstrated that the well-conserved serine nucleophile is essential for the wild-type pathogenic potential of MDV, as evidenced by the fact that the *vLIP* deletion mutant  $\Delta vLIP$  and the serine nucleophile point mutant *vLIP* S307A showed statistically indistinguishable attenuated phenotypes *in vivo* (Tables 2 and 3). The data on *in vivo* replication, survival, and tumor incidence presented in this study all indicate that  $\Delta vLIP$  and *vLIP* S307A are equally attenuated relative to the *vLIP*\*-*rev* revertant virus (Tables 2 and 3; Fig. 7). If the lack of lipase activity observed in assays of *vLIP* protein meant that the lipase homology was irrelevant to *vLIP* function, then we would have expected the serine nucleophile mutant to behave like wild-type virus *in vivo*. Instead, the *in vivo* data indicate that the serine nucleophile mutant *vLIP* S307A and the  $\Delta vLIP$  deletion mutant are equally attenuated relative to revertant virus.

The seemingly paradoxical conservation of significant amino

acid homology to catalytic elements of known lipases in a viral protein that appears to be devoid of conventional lipase activity invites the notion that "tinkering" may be at play in this example of viral homology to a cellular gene. Tinkering explains molecular evolution as a process by which new functions are developed through the modification of preexisting genes rather than through *de novo* invention (42). It is possible that *vLIP* has evolved to use lipase homology in a manner related to the cellular lipase(s) from which it was derived, but no longer as a conventional lipase.

Certain proteins, including a number of examples from herpesviruses, undergo fatty acylation, where myristoyl or palmitoyl fatty acids become covalently attached at specific amino acids through the activity of enzymes that act in *trans* (22, 34, 51, 54, 66). Such modifications usually serve to anchor proteins at intracellular membranes and are often essential to proper protein function (13, 66). The example of *vLIP* might point to an alternative method by which viruses may gain covalent attachment of fatty acids to secreted proteins: via piracy of the host cell lipase gene(s). The  $\alpha/\beta$  hydrolases are understood to employ catalytic strategies similar to those of the serine proteases, such as chymotrypsin (15, 38, 74). Therefore, as  $\alpha/\beta$  hydrolases, the lipases homologous to *vLIP* employ a catalytic mechanism which requires that a stable "acyl enzyme" intermediate be formed, where a fatty acid is left covalently bonded to the serine nucleophile (38). Only once a water molecule is activated to perform a nucleophilic substitution to release the bound fatty acid does the free serine hydroxyl group of the active site become regenerated. Therefore, it is conceivable that the lipase homology of *vLIP* functions in autoacylation rather than in bona fide lipid hydrolysis. In such a scenario, the lipase reaction would stop at the stable acyl enzyme intermediate of the lipase reaction mechanism rather than continuing to perform a complete hydrolysis.

Autoacylation might allow for the targeting of a pathogenic effector function to the plasma membranes of cells, or perhaps to lipoprotein complexes circulating in the blood. The lipid bonding hypothesis is supported by the appearance of cysteines near the *vLIP* nucleophile position. Cysteine is a good nucleophile and is known to accept palmitoyl fatty acids in certain cellular and viral proteins, including the Marburg virus glycoprotein (32, 66). These cysteines are positioned at -4, +6, +10, and +21 relative to the *vLIP* serine nucleophile position (Fig. 2a) and are absolutely conserved among *vLIP* homologues in the MD-like genus as well as in the avian adenoviruses (20, 23, 37, 59, 80). Cysteine residues are not found so close to the nucleophile position in any characterized cellular lipase. However, it is interesting that certain as yet uncharacterized lipase homologues found in the genomes of *Drosophila melanogaster* (NP\_609442) and *Anopheles gambiae* (XP\_319853) share cysteines with *vLIP* at the -4 and +6 positions.

The hypothetical role of the *vLIP* nucleophile in fatty acid bonding will be addressed in future studies, and other explanations may resolve the question of why the *vLIP* S307A serine nucleophile mutant and lipase domain deletion mutants showed very similar, attenuated phenotypes *in vivo*. However, it is worth noting that there are other examples of enzymatically inactive lipase homologues in nature. For instance, PLRP1s conserve appropriate catalytic-triad residues at all three positions and are found alongside PLRP2s and classical

PLs in the gastric juices of all mammals examined to date but do not show any lipase activity *in vitro* (24, 28). Furthermore, several insect yolk proteins are homologous to the pancreatic lipases (14, 69, 76). Although lacking the serine nucleophile and thus catalytically inactive, these yolk proteins are believed to have roles in binding lipid-conjugated steroid hormones to help regulate insect development (14, 69).

While the exact role of vLIP remains unsolved, our data strongly indicate that vLIP provides an advantage for growth *in vivo* but is completely dispensable in cell culture, which may point to a role in immune modulation—especially since the protein is secreted. Furthermore, we have demonstrated that the lipase homologous residues are critical to the pathogenic effector function of vLIP *in vivo*. Since vLIP belongs to a group of lipase-like open reading frames found in several avian adenoviruses and throughout the Marek's disease-like genus of herpesviruses, we offer the first evidence for a direct role in virus replication for this novel family of virus genes.

#### ACKNOWLEDGMENTS

J.P.K. gratefully acknowledges the expert technical assistance of D. R. Robinson, A. Bora Inceoglu, and Arun Bruhn at the University of California, Davis. We thank Martin Messerle (University of Halle, Halle, Germany) for kindly providing recombinant plasmid pST76K-SR and Sanjay Reddy (Texas A&M University, College Station, TX) for cosmid sn5.

The project was supported by the National Research Initiative of the USDA Cooperative State Research, Education, and Extension Service, grant 2004-35204-14653 (awarded to J.P.K.). Additional support was provided by NIH and USDA awards to H.-J.K.

#### REFERENCES

- Adler, H., M. Messerle, M. Wagner, and U. H. Koszinowski. 2000. Cloning and mutagenesis of the murine gammaherpesvirus 68 genome as an infectious bacterial artificial chromosome. *J. Virol.* **74**:6964–6974.
- Afonso, C. L., E. R. Tulman, Z. Lu, E. Oma, G. F. Kutish, and D. L. Rock. 1999. The genome of *Melanoplus sanguinipes* entomopoxvirus. *J. Virol.* **73**:533–552.
- Afonso, C. L., E. R. Tulman, Z. Lu, L. Zsak, D. L. Rock, and G. F. Kutish. 2001. The genome of turkey herpesvirus. *J. Virol.* **75**:971–978.
- Akiyama, Y., and S. Kato. 1974. Two cell lines from lymphomas of Marek's disease. *Biken J.* **17**:105–116.
- Allal, C., C. Buisson-Brenac, V. Marion, C. Claudel-Renard, T. Faraut, P. Dal Monte, D. Streblov, M. Record, and J. L. Davignon. 2004. Human cytomegalovirus carries a cell-derived phospholipase A2 required for infectivity. *J. Virol.* **78**:7717–7726.
- Altschul, S. F., W. Gish, W. Miller, E. W. Myers, and D. J. Lipman. 1990. Basic local alignment search tool. *J. Mol. Biol.* **215**:403–410.
- Altschul, S. F., T. L. Madden, A. A. Schaffer, J. Zhang, Z. Zhang, W. Miller, and D. J. Lipman. 1997. Gapped BLAST and PSI-BLAST: a new generation of protein database search programs. *Nucleic Acids Res.* **25**:3389–3402.
- Baek, S. H., J. Y. Kwak, S. H. Lee, T. Lee, S. H. Ryu, D. J. Uhlinger, and J. D. Lambeth. 1997. Lipase activities of p37, the major envelope protein of vaccinia virus. *J. Biol. Chem.* **272**:32042–32049.
- Bawden, A. L., K. J. Glassberg, J. Diggins, R. Shaw, W. Farmerie, and R. W. Moyer. 2000. Complete genomic sequence of the *Amsacta moorei* entomopoxvirus: analysis and comparison with other poxviruses. *Virology* **274**:120–139.
- Bezzine, S., A. Roussel, J. de Caro, L. Gastinel, A. de Caro, F. Carriere, S. Leydier, R. Verger, and C. Cambillau. 1998. An inactive pancreatic lipase-related protein is activated into a triglyceride-lipase by mutagenesis based on the 3-D structure. *Chem. Phys. Lipids* **93**:103–114.
- Borst, E. M., G. Hahn, U. H. Koszinowski, and M. Messerle. 1999. Cloning of the human cytomegalovirus (HCMV) genome as an infectious bacterial artificial chromosome in *Escherichia coli*: a new approach for construction of HCMV mutants. *J. Virol.* **73**:8320–8329.
- Bourne, Y., C. Martinez, B. Kerfelec, D. Lombardo, C. Chapus, and C. Cambillau. 1994. Horse pancreatic lipase. The crystal structure refined at 2.3 Å resolution. *J. Mol. Biol.* **238**:709–732.
- Boutin, J. A. 1997. Myristoylation. *Cell. Signal.* **9**:15–35.
- Bownes, M. 1992. Why is there sequence similarity between insect yolk proteins and vertebrate lipases? *J. Lipid Res.* **33**:777–790.
- Brady, L., A. M. Brzozowski, Z. S. Derewenda, E. Dodson, G. Dodson, S. Tolley, J. P. Turkenburg, L. Christiansen, B. Huge-Jensen, L. Nørskov, et al. 1990. A serine protease triad forms the catalytic centre of a triacylglycerol lipase. *Nature* **343**:767–770.
- Briquet-Laugier, V., O. Ben-Zeev, and M. H. Doolittle. 1998. Determining lipoprotein lipase and hepatic lipase activity using radiolabeled substrates. *Methods Mol. Biol.* **109**:81–95.
- Calnek, B. W. 2001. Pathogenesis of Marek's disease virus infection. *Curr. Top. Microbiol. Immunol.* **255**:25–55.
- Calnek, B. W., H. K. Addinger, and D. E. Kahn. 1970. Feather follicle epithelium: a source of enveloped and infectious cell-free herpesvirus from Marek's disease. *Avian Dis.* **14**:219–233.
- Calnek, B. W., and R. L. Witter. 1997. Marek's disease, p. 369–413. *In* B. W. Calnek (ed.), *Diseases of poultry*. Iowa State University Press, Ames.
- Cao, J. X., P. J. Krell, and E. Nagy. 1998. Sequence and transcriptional analysis of terminal regions of the fowl adenovirus type 8 genome. *J. Gen. Virol.* **79**:2507–2516.
- Carriere, F., C. Withers-Martinez, H. van Tilbeurgh, A. Roussel, C. Cambillau, and R. Verger. 1998. Structural basis for the substrate selectivity of pancreatic lipases and some related proteins. *Biochim. Biophys. Acta* **1376**:417–432.
- Chung, T. D., J. P. Wymer, M. Kulka, C. C. Smith, and L. Aurelian. 1990. Myristylation and polylysine-mediated activation of the protein kinase domain of the large subunit of herpes simplex virus type 2 ribonucleotide reductase (ICP10). *Virology* **179**:168–178.
- Clavijo, A., P. J. Krell, and E. Nagy. 1996. Molecular cloning and restriction enzyme mapping of avian adenovirus type 8 DNA. *Virus Res.* **45**:93–99.
- Crenon, I., E. Foglizzo, B. Kerfelec, A. Verine, D. Pignol, J. Hermoso, J. Bonicel, and C. Chapus. 1998. Pancreatic lipase-related protein type I: a specialized lipase or an inactive enzyme. *Protein Eng.* **11**:135–142.
- Crenon, I., S. Jayne, B. Kerfelec, J. Hermoso, D. Pignol, and C. Chapus. 1998. Pancreatic lipase-related protein type I: a double mutation restores a significant lipase activity. *Biochem. Biophys. Res. Commun.* **246**:513–517.
- Cui, X., L. F. Lee, W. M. Reed, H. J. Kung, and S. M. Reddy. 2004. Marek's disease virus-encoded vIL-8 gene is involved in early cytolytic infection but dispensable for establishment of latency. *J. Virol.* **78**:4753–4760.
- Cyglér, M., and J. D. Schrag. 1997. Structure as basis for understanding interfacial properties of lipases. *Methods Enzymol.* **284**:3–27.
- De Caro, J., F. Carriere, P. Barboni, T. Giller, R. Verger, and A. De Caro. 1998. Pancreatic lipase-related protein 1 (PLRP1) is present in the pancreatic juice of several species. *Biochim. Biophys. Acta* **1387**:331–341.
- Diaz, B. L., and J. P. Arm. 2003. Phospholipase A(2). *Prostaglandins Leukot. Essent. Fatty Acids* **69**:87–97.
- Egmond, M. R., and C. J. van Bommel. 1997. Impact of structural information on understanding of lipolytic function. *Methods Enzymol.* **284**:119–129.
- Friedman, H. M., L. Wang, N. O. Fishman, J. D. Lambris, R. J. Eisenberg, G. H. Cohen, and J. Lubinski. 1996. Immune evasion properties of herpes simplex virus type 1 glycoprotein gC. *J. Virol.* **70**:4253–4260.
- Funke, C., S. Becker, H. Dartsch, H. D. Klenk, and E. Muhlberger. 1995. Acylation of the Marburg virus glycoprotein. *Virology* **208**:289–297.
- Girod, A., C. E. Wobus, Z. Zadori, M. Ried, K. Leike, P. Tijssen, J. A. Kleinschmidt, and M. Hallek. 2002. The VP1 capsid protein of adeno-associated virus type 2 is carrying a phospholipase A2 domain required for virus infectivity. *J. Gen. Virol.* **83**:973–978.
- Harty, R. N., G. B. Caughman, V. R. Holden, and D. J. O'Callaghan. 1993. Characterization of the myristylated polypeptide encoded by the UL1 gene that is conserved in the genome of defective interfering particles of equine herpesvirus 1. *J. Virol.* **67**:4122–4132.
- Heikinheimo, P., A. Goldman, C. Jeffries, and D. L. Ollis. 1999. Of barn owls and bankers: a lush variety of alpha/beta hydrolases. *Structure Fold Des.* **7**:R141–R146.
- Hennig, H., N. Osterrieder, M. Muller-Steinhardt, H. M. Teichert, H. Kirchner, and K. P. Wandinger. 2003. Detection of Marek's disease virus DNA in chicken but not in human plasma. *J. Clin. Microbiol.* **41**:2428–2432.
- Hess, M., H. Blocker, and P. Brandt. 1997. The complete nucleotide sequence of the egg drop syndrome virus: an intermediate between mastadenoviruses and aviadenoviruses. *Virology* **238**:145–156.
- Holmquist, M. 2000. Alpha/beta-hydrolase fold enzymes: structures, functions and mechanisms. *Curr. Protein Pept. Sci.* **1**:209–235.
- Isfort, R., D. Jones, R. Kost, R. Witter, and H. J. Kung. 1992. Retrovirus insertion into herpesvirus *in vitro* and *in vivo*. *Proc. Natl. Acad. Sci. USA* **89**:991–995.
- Iyer, S. S., J. A. Barton, S. Bourgoin, and D. J. Kusner. 2004. Phospholipases D1 and D2 coordinately regulate macrophage phagocytosis. *J. Immunol.* **173**:2615–2623.
- Izumiya, Y., H. K. Jang, M. Ono, and T. Mikami. 2001. A complete genomic DNA sequence of Marek's disease virus type 2, strain HPRS24. *Curr. Top. Microbiol. Immunol.* **255**:191–221.
- Jacob, F. 1977. Evolution and tinkering. *Science* **196**:1161–1166.
- Jarosinski, K. W., R. Yunis, P. H. O'Connell, C. J. Markowski-Grimsrud, and K. A. Schat. 2002. Influence of genetic resistance of the chicken and

- virulence of Marek's disease virus (MDV) on nitric oxide responses after MDV infection. *Avian Dis.* **46**:636–649.
44. **Jennens, M. L., and M. E. Lowe.** 1994. A surface loop covering the active site of human pancreatic lipase influences interfacial activation and lipid binding. *J. Biol. Chem.* **269**:25470–25474.
  45. **Jones, D. T.** 1999. GenTHREADER: an efficient and reliable protein fold recognition method for genomic sequences. *J. Mol. Biol.* **287**:797–815.
  46. **Kingham, B. F., V. Zelnik, J. Kopacek, V. Majerciak, E. Ney, and C. J. Schmidt.** 2001. The genome of herpesvirus of turkeys: comparative analysis with Marek's disease viruses. *J. Gen. Virol.* **82**:1123–1135.
  47. **Kozak, M.** 1987. At least six nucleotides preceding the AUG initiator codon enhance translation in mammalian cells. *J. Mol. Biol.* **196**:947–950.
  48. **Kozak, M.** 1986. Point mutations define a sequence flanking the AUG initiator codon that modulates translation by eukaryotic ribosomes. *Cell* **44**:283–292.
  49. **Lee, L. F., P. Wu, D. Sui, D. Ren, J. Kamil, H. J. Kung, and R. L. Witter.** 2000. The complete unique long sequence and the overall genomic organization of the GA strain of Marek's disease virus. *Proc. Natl. Acad. Sci. USA* **97**:6091–6096.
  50. **Lin, A. W., C. C. Chang, and C. C. McCormick.** 1996. Molecular cloning and expression of an avian macrophage nitric-oxide synthase cDNA and the analysis of the genomic 5'-flanking region. *J. Biol. Chem.* **271**:11911–11919.
  51. **Loomis, J. S., J. B. Bowzard, R. J. Courtney, and J. W. Wills.** 2001. Intracellular trafficking of the UL11 tegument protein of herpes simplex virus type 1. *J. Virol.* **75**:12209–12219.
  52. **Lowe, M. E.** 1992. The catalytic site residues and interfacial binding of human pancreatic lipase. *J. Biol. Chem.* **267**:17069–17073.
  53. **Lupiani, B., L. F. Lee, X. Cui, I. Gimeno, A. Anderson, R. W. Morgan, R. F. Silva, R. L. Witter, H. J. Kung, and S. M. Reddy.** 2004. Marek's disease virus-encoded Meq gene is involved in transformation of lymphocytes but is dispensable for replication. *Proc. Natl. Acad. Sci. USA* **101**:11815–11820.
  54. **MacLean, C. A., B. Clark, and D. J. McGeoch.** 1989. Gene UL11 of herpes simplex virus type 1 encodes a virion protein which is myristylated. *J. Gen. Virol.* **70**:3147–3157.
  55. **McDermott, M., M. J. Wakelam, and A. J. Morris.** 2004. Phospholipase D. *Biochem. Cell Biol.* **82**:225–253.
  56. **Nardini, M., and B. W. Dijkstra.** 1999. Alpha/beta hydrolase fold enzymes: the family keeps growing. *Curr. Opin. Struct. Biol.* **9**:732–737.
  57. **Nielsen, H., J. Engelbrecht, S. Brunak, and G. von Heijne.** 1997. Identification of prokaryotic and eukaryotic signal peptides and prediction of their cleavage sites. *Protein Eng.* **10**:1–6.
  58. **Nielsen, H., J. Engelbrecht, S. Brunak, and G. von Heijne.** 1997. A neural network method for identification of prokaryotic and eukaryotic signal peptides and prediction of their cleavage sites. *Int. J. Neural Syst.* **8**:581–599.
  59. **Ojkic, D., and E. Nagy.** 2000. The complete nucleotide sequence of fowl adenovirus type 8. *J. Gen. Virol.* **81**:1833–1837.
  60. **Oliver, K. G., R. M. Buller, P. J. Hughes, J. W. Putney, Jr., and G. J. Palumbo.** 1992. Inhibition of agonist-induced activation of phospholipase C following poxvirus infection. *J. Biol. Chem.* **267**:25098–25103.
  61. **Ollis, D. L., E. Cheah, M. Cygler, B. Dijkstra, F. Frolov, S. M. Franken, M. Harel, S. J. Remington, I. Silman, J. Schrag, et al.** 1992. The alpha/beta hydrolase fold. *Protein Eng.* **5**:197–211.
  62. **Palumbo, G. J., W. C. Glasgow, and R. M. Buller.** 1993. Poxvirus-induced alteration of arachidonate metabolism. *Proc. Natl. Acad. Sci. USA* **90**:2020–2024.
  63. **Parcells, M. S., S. F. Lin, R. L. Dienglewicz, V. Majerciak, D. R. Robinson, H. C. Chen, Z. Wu, G. R. Dubyak, P. Brunovskis, H. D. Hunt, L. F. Lee, and H. J. Kung.** 2001. Marek's disease virus (MDV) encodes an interleukin-8 homolog (vIL-8): characterization of the vIL-8 protein and a vIL-8 deletion mutant MDV. *J. Virol.* **75**:5159–5173.
  64. **Petherbridge, L., A. C. Brown, S. J. Baigent, K. Howes, M. A. Sacco, N. Osterrieder, and V. K. Nair.** 2004. Oncogenicity of virulent Marek's disease virus cloned as bacterial artificial chromosomes. *J. Virol.* **78**:13376–13380.
  65. **Reddy, S. M., B. Lupiani, I. M. Gimeno, R. F. Silva, L. F. Lee, and R. L. Witter.** 2002. Rescue of a pathogenic Marek's disease virus with overlapping cosmid DNAs: use of a pp38 mutant to validate the technology for the study of gene function. *Proc. Natl. Acad. Sci. USA* **99**:7054–7059.
  66. **Resh, M. D.** 1999. Fatty acylation of proteins: new insights into membrane targeting of myristoylated and palmitoylated proteins. *Biochim. Biophys. Acta* **1451**:1–16.
  67. **Roussel, A., J. de Caro, S. Bezzine, L. Gastinel, A. de Caro, F. Carriere, S. Leydier, R. Verger, and C. Cambillau.** 1998. Reactivation of the totally inactive pancreatic lipase RP1 by structure-predicted point mutations. *Proteins* **32**:523–531.
  68. **Sambrook, J., E. F. Fritsch, and T. Maniatis.** 1989. *Molecular cloning: a laboratory manual*, 2nd ed. Cold Spring Harbor Laboratory Press, Cold Spring Harbor, N.Y.
  69. **Sappington, T. W.** 2002. The major yolk proteins of higher Diptera are homologs of a class of minor yolk proteins in lepidoptera. *J. Mol. Evol.* **55**:470–475.
  70. **Schrag, J. D., and M. Cygler.** 1997. Lipases and alpha/beta hydrolase fold. *Methods Enzymol.* **284**:85–107.
  71. **Schrag, J. D., F. K. Winkler, and M. Cygler.** 1992. Pancreatic lipases: evolutionary intermediates in a positional change of catalytic carboxylates? *J. Biol. Chem.* **267**:4300–4303.
  72. **Schumacher, D., B. K. Tischer, W. Fuchs, and N. Osterrieder.** 2000. Reconstitution of Marek's disease virus serotype 1 (MDV-1) from DNA cloned as a bacterial artificial chromosome and characterization of a glycoprotein B-negative MDV-1 mutant. *J. Virol.* **74**:11088–11098.
  73. **Spiegel, S., D. Foster, and R. Kolesnick.** 1996. Signal transduction through lipid second messengers. *Curr. Opin. Cell Biol.* **8**:159–167.
  74. **Stryer, L.** 1995. Catalytic strategies, p. 207–237. *In Biochemistry*, 4th ed. W. H. Freeman, New York, N.Y.
  75. **Svendsen, A.** 2000. Lipase protein engineering. *Biochim. Biophys. Acta* **1543**:223–238.
  76. **Terpstra, P., and G. Ab.** 1988. Homology of *Drosophila* yolk proteins and the triacylglycerol lipase family. *J. Mol. Biol.* **202**:663–665.
  77. **Tjoelker, L. W., C. Eberhardt, J. Unger, H. L. Trong, G. A. Zimmerman, T. M. McIntyre, D. M. Stafforini, S. M. Prescott, and P. W. Gray.** 1995. Plasma platelet-activating factor acetylhydrolase is a secreted phospholipase A2 with a catalytic triad. *J. Biol. Chem.* **270**:25481–25487.
  78. **Tulman, E. R., C. L. Afonso, Z. Lu, L. Zsak, D. L. Rock, and G. F. Kutish.** 2000. The genome of a very virulent Marek's disease virus. *J. Virol.* **74**:7980–7988.
  79. **van Tilbeurgh, H., M. P. Egloff, C. Martinez, N. Rugani, R. Verger, and C. Cambillau.** 1993. Interfacial activation of the lipase-procolipase complex by mixed micelles revealed by X-ray crystallography. *Nature* **362**:814–820.
  80. **Washietl, S., and F. Eisenhaber.** 2003. Reannotation of the CELO genome characterizes a set of previously unassigned open reading frames and points to novel modes of host interaction in avian adenoviruses. *BMC Bioinformatics* **4**:55.
  81. **Winkler, F. K., A. D'Arcy, and W. Hunziker.** 1990. Structure of human pancreatic lipase. *Nature* **343**:771–774.
  82. **Withers-Martinez, C., F. Carriere, R. Verger, D. Bourgeois, and C. Cambillau.** 1996. A pancreatic lipase with a phospholipase A1 activity: crystal structure of a chimeric pancreatic lipase-related protein 2 from guinea pig. *Structure* **4**:1363–1374.
  83. **Witter, R. L.** 1983. Characteristics of Marek's disease viruses isolated from vaccinated commercial chicken flocks: association of viral pathotype with lymphoma frequency. *Avian Dis.* **27**:113–132.
  84. **Witter, R. L.** 1997. Increased virulence of Marek's disease virus field isolates. *Avian Dis.* **41**:149–163.